

EES Catalysis

Accepted Manuscript

This article can be cited before page numbers have been issued, to do this please use: S. Shukla, V. K. Jose and N. Mathews, *EES. Catal.*, 2024, DOI: 10.1039/D4EY00091A.



This is an Accepted Manuscript, which has been through the Royal Society of Chemistry peer review process and has been accepted for publication.

Accepted Manuscripts are published online shortly after acceptance, before technical editing, formatting and proof reading. Using this free service, authors can make their results available to the community, in citable form, before we publish the edited article. We will replace this Accepted Manuscript with the edited and formatted Advance Article as soon as it is available.

You can find more information about Accepted Manuscripts in the [Information for Authors](#).

Please note that technical editing may introduce minor changes to the text and/or graphics, which may alter content. The journal's standard [Terms & Conditions](#) and the [Ethical guidelines](#) still apply. In no event shall the Royal Society of Chemistry be held responsible for any errors or omissions in this Accepted Manuscript or any consequences arising from the use of any information it contains.

Shining Light on Hybrid Perovskites for Photoelectrochemical Solar to Fuel Conversion

Sudhanshu Shukla, Vishal Jose, Nripan Mathews

Broader Context:

Fossil fuel-dependent growth has led to an unprecedented rise in atmospheric CO₂ levels. This has triggered climate change which emerged as one of the biggest global challenges of our time. A paradigm shift to renewable energy is urgently required to decarbonize the economy and ensure carbon-neutral and sustainable growth. Artificial photosynthetic systems, inspired by natural photosynthesis, have garnered tremendous interest in the spontaneous generation of value-added chemical fuels from CO₂ and water entirely from solar energy. Halide perovskites have emerged as a promising material system for photoelectrocatalysis, after their resounding success in photovoltaics. The versatile properties of halide perovskites unlock the key to facilitating many important catalytic reactions, beyond CO₂ conversion. This perspective provides a comprehensive and critical assessment of the potential of cost-competitive halide perovskite-based photocatalytic systems. We intend to bring the research community's interest for driving value-added catalytic reactions using halide perovskite. By doing so, we identify fundamental issues that require immediate attention and provide clear future directions that must be considered for this technology to become a commercial reality and make impact tangible impact.



Shining Light on Hybrid Perovskites for Photoelectrochemical Solar to Fuel Conversion

[View Article Online](#)

DOI: 10.1039/D4CY00091A

Sudhanshu Shukla^{1,2,3*}, *Vishal Jose*^{1,2,3}, *Nripan Mathews*^{4,5*}

¹Imec, imo-imomec, Thor Park 8320, 3600 Genk, Belgium.

²EnergyVille, imo-imomec, Thor Park 8320, 3600 Genk, Belgium.

³Hasselt University, imo-imomec, Martelarenlaan 42, 3500 Hasselt, Belgium.

⁴School of Materials Science and Engineering, Nanyang Technological University, Singapore 639798.

⁵Energy Research Institute @ NTU, Nanyang Technological University, Research Techno Plaza, 50 Nanyang Drive, Singapore 637553.



Abstract

View Article Online
DOI: 10.1039/D4EY00091A

Hybrid halide perovskites (HaPs) represent a class of material with excellent optoelectronic properties providing distinct avenues for disruptive photo(-electro) catalytic technologies. However, their photocatalytic activity, selectivity and stability remains a scientific and technological hurdle. In this perspective, we discuss fundamental aspects of perovskite based photocatalytic systems, specifically for CO₂ conversion and high value oxidation reactions, and highlight critical limiting factors and on-going challenges in the field. We critically assess the recent advances in designing halide perovskite hetero-interfaces and characterization methodologies which are often used to define the performance metrics. Further, we outline important questions and identify emerging trends in relation to the remediation strategy towards improved photocatalytic performance and stability from halide perovskite semiconductors.



Introduction

Fossil fuels dependent growth has led to an unprecedented rise in the atmospheric CO₂ levels. This has triggered a climate emergency which has emerged as one of the biggest global challenges of our time.¹ Therefore, a paradigm shift to renewable energy is urgently required to meet global energy demands and ensure sustainable growth in a cost-effective manner.² Two dominant factors are fueling the rapidly transforming renewable energy landscape– (i) decrease in the levelized cost of electricity (LCOE) of photovoltaics,³ and (ii) heavy reliance on fossil-based resources to generate liquid fuels for transportation and chemical feedstocks for high value synthetic chemicals in fertilizer and pharmaceutical industries.⁴ While falling PV prices are favorable for ever increasing energy demands, the associated intermittency related to diurnal changes and climatic variations pose a limit to its applicability, especially in hard to decarbonize sectors such as transportation.⁵ Thus, renewable technologies aiming to convert CO₂ and store energy in the form of synthetic fuels and value-added chemicals are highly desirable to not only develop alternative sustainable fuels but to close the carbon cycle.

Solar-driven photo(electro)catalysis systems, inspired from natural photosynthesis, enable spontaneous generation of high energy density and value-added chemical fuels from CO₂ and water, also known as artificial photosynthesis, solar fuels, and carbon-capture, and utilization (CCU).⁶ The energy density (per unit weight or volume) of photoelectrochemically produced molecules is higher than conventionally used lithium batteries, making it suitable for long-term storage and mobility.⁷ Thus, offering a clean, cost-competitive, and flexible alternative to current fossil-fuel based technologies for sustainable intersectoral societal growth.

The idea of renewably sourced chemicals from CO₂ recycling has intrigued researchers for decades, since the first demonstration of photocatalytic water splitting on semiconducting TiO₂ surface from Honda and Fujishima⁸ and later, photoelectrochemical CO₂ reduction using p-



GaP semiconductor from Halmann.⁹ Since then, strides have been made in photocatalytic water splitting in terms of efficiency and scale.¹⁰ In contrast, the progress in photoelectrochemical CO₂ reduction remained limited due to complexities associated with solvation dynamics, activation barrier, reaction kinetics (multiple electron and proton transfer processes), preferential dimerization, material stability in aqueous media and difficulties related to up-scaling. Moreover, the interference of impurities and spurious carbon signals renders unreliable quantification of product distribution from photocatalytic CO₂ reduction.¹¹

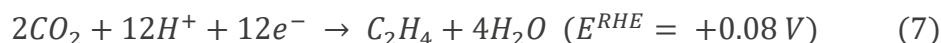
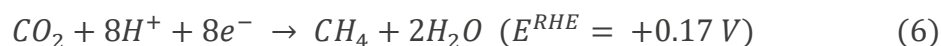
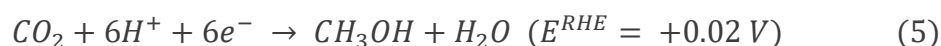
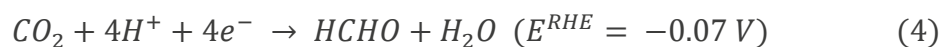
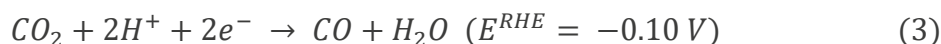
Halide perovskites (HaP) have emerged as low-cost, easy processable semiconductors with intriguing properties like long charge-carrier diffusion lengths and bandgap tunability and direct optical excitation with strong absorption coefficients ($> 10^5 \text{ cm}^{-1}$). With 26.54% certified power conversion efficiency,¹² HaPs based solar cells have outcompeted many established thin film photovoltaic technologies in just 10 years. In parallel, the versatile properties of HaPs place them at the forefront of photocatalysis. For the first time, a HaP was exploited for conducting photocatalytic CO₂ reduction by Y.-F. Xu *et al.*, in 2017.¹³ The authors utilized CsPbBr₃ QDs and its composites with graphene oxide for artificial CO₂ reduction in ethyl acetate solvent, where the pristine QDs demonstrated an average electron consumption rate of 23.7 $\mu\text{mol g}^{-1} \text{ h}^{-1}$. From then multiple works were conducted to improve the efficiency, selectivity, and stability of various HaPs in organic and inorganic solvents along with shedding light on reaction mechanisms and material degradation processes. For instance, recently, L. Ding and co-workers revealed the CO₂ reduction potential of Cs₂AgBiBr₆ QDs encapsulated in a metal organic framework by attaining CO production rates of 309.01 $\mu\text{mol g}^{-1} \text{ h}^{-1}$.¹⁴ However, selectivity of these materials are still primarily limited to CO and CH₄, unlike materials such as carbon nitride that could selectively generate higher order carbon products. For example, C₂H₆ evolution rate of 616.6 $\mu\text{mol g}^{-1} \text{ h}^{-1}$,¹⁵ and CH₃OH evolution rate of 13.9

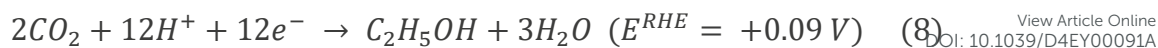


$\mu\text{mol g}^{-1} \text{h}^{-1}$.¹⁶ Profound advancements are made in tailoring and employing HaPs for various redox reactions and chemical valorisation.

1. Considerations and fundamental challenges for driving key photoelectrochemical reactions: There is plenty of room for perovskites

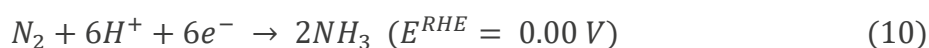
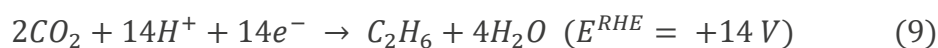
Several high energy density and value-added compounds can be targeted through photoelectrochemical reduction of environmental feedstocks such as water, CO₂ (hydrocarbons), and N₂ to obtain hydrogen, hydrocarbons and ammonia, respectively. For instance, CO₂ can be reduced and converted to obtain several high energy densities and value-added gaseous and liquid C₁ (such as CO, methane, methanol, formic acid) and C₂₊ (such as ethylene, ethanol, propanol, ethylene glycol) chemical products.¹⁷ Thermodynamically, CO₂ reduction is an energy demanding reaction. The energy required to break C—O bond is ~ 750 KJ/mol. This is slightly higher than to electrochemical potential required for hydrogen evolution reaction (HER) (~ 237 KJ/mol). However, kinetic factors related to CO₂ activation barrier, and complex multi-step reaction pathways push the energetics well above the thermodynamic limit, giving rise to electrochemical overpotential.¹⁸ Similarly N₂ can be converted to NH₃, although poses higher challenge due to high energy required to break strong N—N bond. Standard reduction potentials (vs RHE) and typical products are given below for various reactions involving electron and proton transfers:^{19, 20}





View Article Online

DOI: 10.1039/D4EY00091A



Oxidation reduction:



Therefore, the fundamental limitation arises from the overall voltage requirement imposed by thermodynamics and kinetics. Typically, the other half of the reduction reaction is generally coupled to the oxidation reaction, namely oxygen evolution reaction (OER). From the above mentioned overpotential losses, the cumulative voltage requirement for coupled HER-OER or CO₂R-OER reaction exceeds beyond 1.8 V. Figure 1 a represent the typical reduction (in blue) and oxidation (in black) reactions performed at the photocathode and photoanode respectively. Thus, the choice of anodic reaction is not merely limited to OER. There are alternative oxidation reactions (AOR) such as - iodide oxidation, glycerol oxidation, plastic and biomass oxidation, degradation of organic pollutants, selective organic transformation.²¹ These are useful to obtain high value chemical compounds with overall less voltage requirement.

The input energy for endergonic reduction can be provided by the photocatalyst (an irradiated semiconductor in direct contact with the reactants) in the form of photovoltage. The fundamental principle behind a Photo(electro)catalytic process consists of (i) efficient absorption of photons followed by the generation of electron hole pairs, (ii) carrier separation and transport to the surface, and (iii) electrochemical reduction or oxidation reaction involving electrons from the conduction band or holes from the valence band.²² The overall photocurrent of the process can be expressed as:

$$J = J_{abs} \times \eta_{trans} \times \eta_{FE} \quad (9)$$

Where J_{abs} is the photocurrent due to the absorbed photons, η_{trans} is charge transfer (or separation) efficiency, η_{FE} and is the Faradaic efficiency (catalysis process). Optimization of



each of these parameters requires holistic materials optimization, interface engineering and control over surface chemistry.

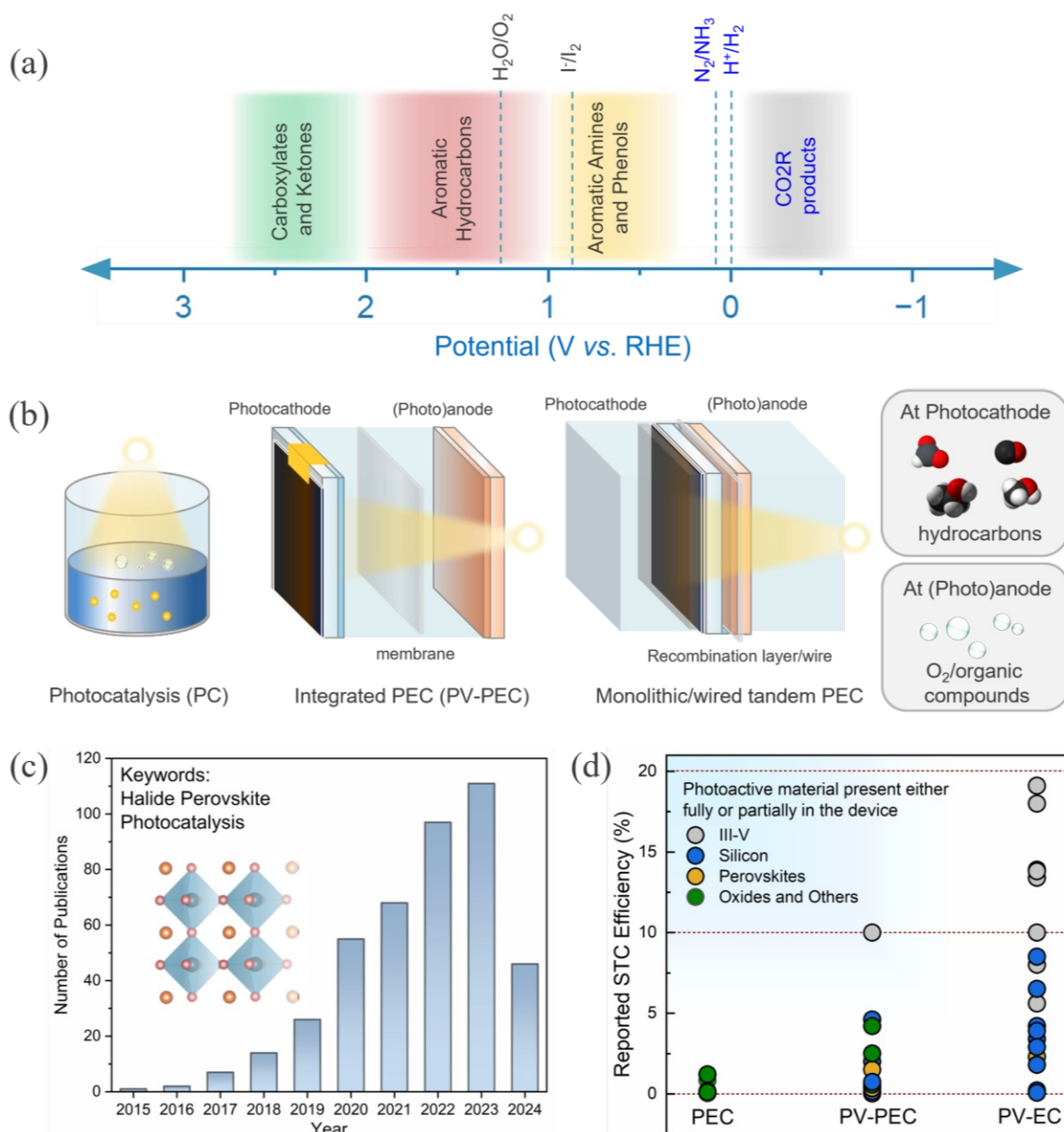


Figure 1. (a) Common reduction and Organic oxidation reactions are depicted over potential ranges.^{20, 21, 23, 24} (b) Different architecture and corresponding components of a PC, integrated PV-PEC and monolithic/wired tandem PEC device. PEC devices are configured with at least one photoelectrode (photocathode with anode or photoanode with cathode) and integrated PEC may have a wired connected PV component. (c) Trends in publications on halide perovskite related papers on photoelectrocatalysis for the period 2015 to 2024 (source: Scopus; keyword:



halide perovskite and photocatalysis, assessed on 25 April 2024). (c) Reported solar-to-carbon (STC) efficiency for different device architectures using various photoactive materials.²⁵⁻⁵⁶

Hence photocurrent and photovoltage are two critical parameters that determine the overall efficiency. Subsequent sections in the article describe how these two parameters can be optimized.

It is essential to consider different routes⁵⁷ that are used to accomplish HaP driven photoelectrochemical CO₂R: (1) photocatalysis (PC), (2) photoelectrocatalysis (PEC), and photovoltaic integrated PEC (PV-PEC) or buried junction PEC, and (3) tandem PEC scheme as depicted in Figure 1b. Alternatively, PV powered electrolysis (PV-EC) is also a viable way to accomplish CO₂R through electrolysis. However, we will keep our focus on direct and integrated approaches in this perspective. A good account of latest summary on perovskite-based PV-EC can be found in the ref.⁵⁸ Recently, there has been a surge in research activities on HaPs for photo(electro)catalysis, evident from rapidly growing trend of the publications in this field (Figure 1c). Figure 1d depicts a comparative view of the solar to carbon (STC) efficiency for different device architectures and material systems. It becomes clear that STC efficiencies for PEC and PV-PECs are well below 10 % for most of the materials. It is straightforward to envisage above 10 % STC from HaPs devices, considering comparable optoelectronic properties can be achieved for HaPs as for III-V semiconductor (GaAs).

Inorganic metal oxides such as TiO₂, WO₃, ZnO, and α -Fe₂O₃ appeared as early adopters for photocatalytic systems, benefiting from high electronegativity of oxygen, versatile metal-oxygen chemistry, and economic viability.⁵⁹⁻⁶¹ The ionic character of the bonds between the metal and oxygen atomic orbitals results in stable compounds with sufficiently large bandgaps, that typically straddle the redox potentials of various reduction (CO₂, H⁺) and oxidation reactions (water, ethylene glycol, 5-hydroxymethylfurfural). However, the wide bandgap of these materials limits the spectral range of optical absorption, and they suffer from high



recombination losses due to plethora of point defects and polaron formation, severely limiting the availability of carriers for photocatalysis.⁶² Beyond oxides, transition metal dichalcogenides (TMDs) have garnered significant attention for photocatalysis, exhibiting superior optoelectronic properties such as optical absorption, charge transport and rich defect chemistry.⁶³⁻⁶⁶ However, the number of chalcogenides with sufficiently high bandgap is relatively small and, in addition, there are aggravated instability concerns related to photocorrosion in aqueous media.^{65, 67}

Halide perovskites (HaPs) have emerged as a promising class of materials for a wide variety of optoelectronic applications; solar cells,⁶⁸ photodetectors,⁶⁹ light-emitting diodes (LED),⁷⁰ lasers,⁷¹ memristors,⁷² and photoelectrocatalysis.⁷³ The rapid evolution of HaP based devices and their performance is underpinned by their exceptional optoelectronic properties such as defect tolerance, direct bandgap with high optical absorption and ambipolar transport with long-range balanced diffusion lengths. Carrier diffusion lengths, given by $L_D = \sqrt{D\tau}$, of up to 1 μm have been observed, manifesting the low defect density in HaPs. Another feature associated with the defect or disorder induced band tailing is the Urbach energy (E_u). The significantly low value of Urbach energy ($\sim 15 - 30$ meV) is a manifestation of superior optoelectronic quality of HaPs, compared to conventional semiconductors (> 30 meV).⁷⁴ A gamut of unique properties of HaPs stems from its high degree of compositional flexibility and tuneability of structure, dimension, and electronic properties. The structure of perovskites can be easily engineered, beyond archetypal MAPbI_3 , to yield a variety of inorganic-organic hybrids and purely inorganic systems, and facile dimensional tailoring enables realization of 3D, 2D, 1D, 0D, and even mixed dimensional HaPs.^{75, 76} This allows band gap tuneability in wide spectral range (from ultraviolet to near infrared) and control over energy band alignment for favorable energetics. Considering above properties, HaPs seemingly satisfy the key requirements for photocatalytic devices by ensuring efficient optical absorption of photons,



electron-hole pair generation, loss-less carrier transport, and seamless utilization of carriers at the interface to drive redox reactions with sufficiently high rates. However, one of the major limitations that has kept its potential untapped is their aqueous stability, and achieving product selectivity beyond C_1 (CO , CH_4) compounds. This requires more understanding of several unexplored elements related to composition, morphology, charge separation, passivation, and catalytically active sites in HaPs. The development of HaPs based photocatalyst relies on improving optoelectronic as well as photocatalytic properties and mechanistic insights on the underlying descriptors. We discuss important factors governing the photocatalytic activity of HaPs and present methodologies to gain fundamental understanding, as shown in Figure 2.

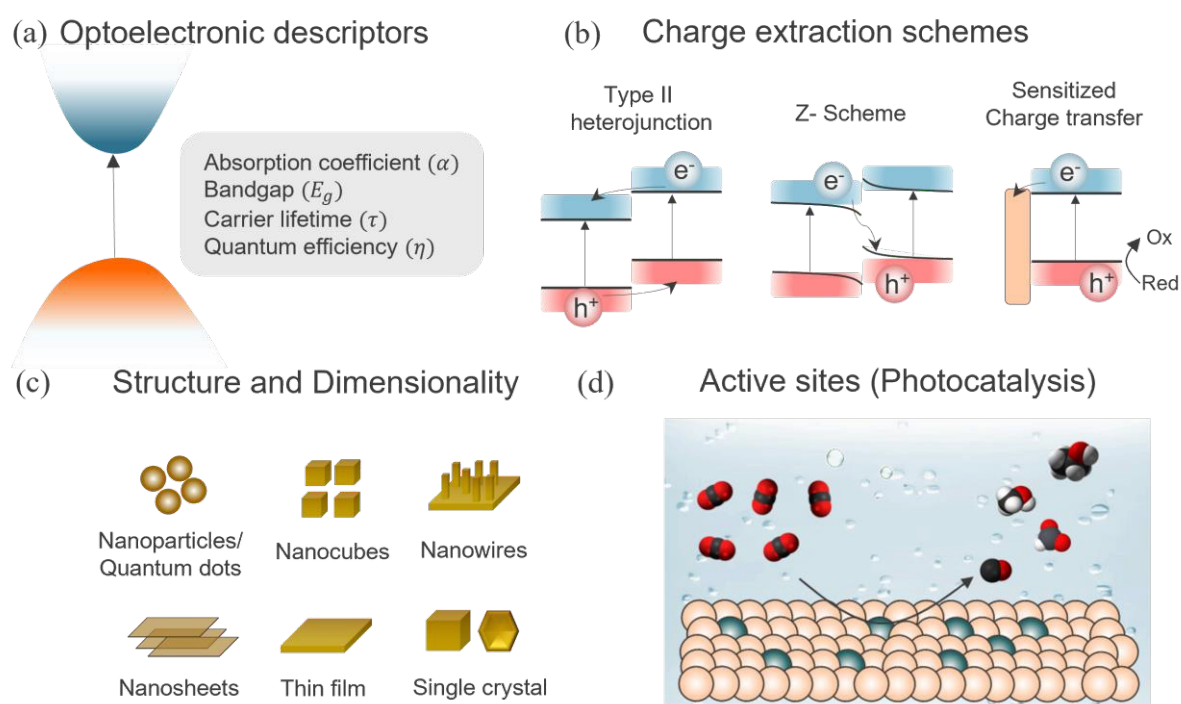


Figure 2. Overview of the themes covered in this perspective. (a) Perovskite band structure and key optoelectronic properties, (b) different heterojunction schemes for efficient charge transfer, (c) Influence of different morphology and dimensionality and (d) the role of surface chemistry in defining the catalytically active site.

In this perspective, we identify the mechanistic challenges that need to be addressed and discuss potential routes to advance the field and rationalize the role that perovskites can play in the



abatement of CO₂ emissions and facilitate its solar driven conversion to value-added chemicals and sustainable fuels.

2. Optoelectronic Aspects of Halide Perovskite based Photocatalytic System

The excellent optoelectronic properties of HaPs are due to their peculiar crystallographic structure and electronic structure. The general formula for perovskite is ABX₃, where A site is typically occupied by a monovalent organic/inorganic cation (CH₃NH₃⁺ or Cs⁺), B is a divalent metal (Pb²⁺, Sn²⁺), and X is a single or mixed halide anion (I⁻, Br⁻, Cl⁻). The structure remains stable for a wide range of small (Cs⁺) and large cation sizes (CH₃NH₃⁺), governed by empirical Goldschmidt tolerance factor.⁷⁷ The bandgap is formed primarily due to the hybridization between metal (B) and halide (X) orbitals.

The valence band maximum (VBM) is dominated by the X p characteristics (with some B s contribution) and conduction band minimum (CBM) is derived from π antibonding of B p and X p orbitals. A cation seems to primarily behave as a spacer and does not directly contribute to the electronic structure but influences the bandgap *via* lattice deformations. Thus, the direct bandgap along with favorable p \rightarrow p transition are the key factors behind high optical absorption in HaPs.⁶⁸ Notably, strong spin-orbit coupling (SOC), due to the presence of heavy metals (like Pb), have been shown to influence the optical transition and carrier lifetime due to Rashba splitting of the CBM.⁷⁸⁻⁸⁰

Broad spectral tunability and different bandgaps can be achieved by facile halide substitution and varying compositions of HaPs, as shown in Figure 3 a. The conduction band position for most of the perovskites is sufficiently negative relative to the redox potential of water splitting, CO₂R and N₂ reduction reaction (N₂RR),⁸¹ providing the driving force to facilitate these reactions. The conduction band position can be varied through halide substitution to selectively match the redox potential. It is also evident that some HaPs have valence band position positive enough to make them suitable for water oxidation and even for high value oxidation reactions



like HMF and ethylene glycol oxidation.²¹ HaPs are mostly investigated as photocatalysts for reduction reaction which is commonly coupled to water oxidation reaction. The photoexcited electrons in the conduction band reduce CO₂, while the holes in the valence band are consumed in H₂O oxidation generating oxygen. Water also acts as a source of protons for hydrogenation of photocatalyzed CO₂, in addition to serving as reducing agent.

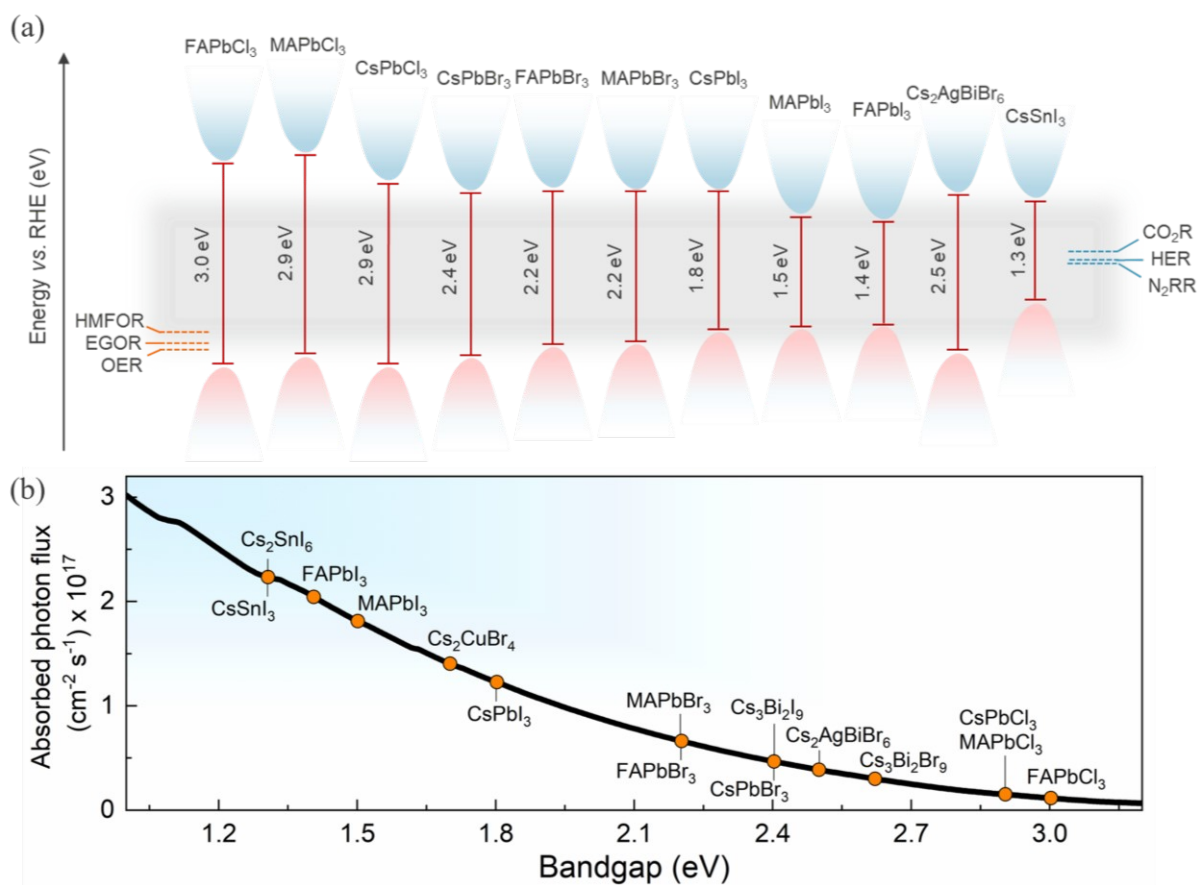


Figure 3. (a) Valence and conduction band positions of selected HaPs with respect to relevant redox cathodic and anodic reactions.^{82, 83} (b) AM1.5G equivalent steady-state absorbed photon flux available for different bandgap HaPs (assuming step-function-like absorptivity) representing their light absorption ability.

In practice, a combination of photocatalysts is more conducive for optimum light absorption, as shown in Figure 3 b, while maintaining the necessary photochemical potential higher than the redox potential. This is generally achieved by forming heterostructures.



2.1 Photophysical and Charge Transfer Processes in Halide Perovskites

Upon irradiation of light above or equal to the bandgap, photoexcited electron-hole pairs are generated and migrate to the surface primarily through diffusion. Drift transport is believed to be less important in perovskites, as the electric fields are screened by the presence of moving ions.⁸⁴ During the migration, carriers undergo various photophysical radiative and/or non-radiative recombination processes due to the presence of disorder, shallow traps, and deep defects. The lower defect density in HaPs ensures long carrier diffusion lengths, implying a reasonably high carrier recombination lifetime and mobilities. Since photoelectrochemical reactions are kinetically slow processes, the photoexcited carrier lifetime must be long enough to ensure the availability of carriers at the surface for redox reactions (Figure 4a).⁸⁵ Thus, charge carrier lifetime (τ) is the most essential descriptor to describe the photocatalytic ability associated with its optoelectronic quality. Determination of carrier lifetime has mostly relied on the photoluminescence (PL) based measurements. Figure 4 a show the carrier lifetime values reported in the literature and corresponding regime for various HaPs, deduced from photoluminescence measurements. Apart from PL, other transient techniques such as – time resolved microwave conductivity (TRMC), optical pump THz probe (OPTP) spectroscopy, transient absorption spectroscopy (TAS), transient photovoltage (TPV) and photoconductivity measurements, have also proven to be quite useful in lifetime assessment.⁸⁶⁻⁸⁸ For instance, Chen *et al.* revealed a long carrier lifetime of up to 30 μ s and 2.7 ms for MAPbI₃ polycrystalline film and MAPbBr₃ single crystal respectively, from steady-state photoconductivity and Hall measurements.⁸⁹ Brenes *et al.* observed a carrier lifetime of 32 μ s in the passivated MAPbI₃ thin films from TRMC measurements.⁹⁰



Photophysical processes like – trap assisted recombination, Shockley-Read-Hall (SRH) recombination, and surface or interface recombination reduce the carrier lifetime and manifest as a change in decay dynamics of transient PL. All these processes are usually concealed in the carrier decay dynamics. While it is straightforward to deduce lifetimes from transient profiles, it is hardly possible to discern underlying physical recombination processes without fluence dependent measurements and an appropriate model.⁹¹ The identification of the lifetime limiting process is imperative to develop focused passivation strategies and enhance the carrier lifetime. Several strategies ranging from doping and alloying,⁹² nanostructuring,^{93, 94} bulk and passivation,⁹⁵⁻⁹⁹ and dimensional tailoring,¹⁰⁰⁻¹⁰² have been demonstrated to enhance the lifetime of carriers in HaPs. Lessons from photovoltaics could be extremely useful to design passivation strategies and harness the photocatalytic activity from enhanced carrier lifetimes. Next to long carrier lifetimes, charge carrier extraction is extremely important for efficient functioning of a photocatalytic device. Charge carrier separation is achieved through different heterojunction schemes, as shown in Figure 4 b. The common heterojunction charge transfer schemes are – Schottky junction, type II heterojunction, Z- Scheme heterojunction (direct and mediated), molecular sensitization. Heterojunction layers commonly serve the dual role of passivation and carrier selective transport layer.¹⁰³⁻¹⁰⁵ It is shown that despite long carrier diffusion lengths, carrier collection can be limited by unoptimized, and low mobility charge transport layers.¹⁰⁶ The charge transfer from perovskites reduces the carrier density within perovskite absorber, therefore the concomitant drop in the PL intensity can act as a qualitative descriptor of the transfer kinetics. Consequently, transient PL has been exploited as a quantitative method to analyze recombination and charge transfer kinetics. This is evident from the reduction in PL lifetimes for CsPbBr₃/Au (Schottky),¹⁰⁷ CsPbBr₃/[Ni(tertpy)₂]²⁺ (molecular sensitizer),¹⁰⁸ Cs₂SnI₆/SnS₂ (type II),¹⁰⁹ CsPbBr₃/TiO₂ (Z-scheme),¹¹⁰ FAPbBr₃/α-Fe₂O₃ (Z-scheme),¹¹¹ CsPbBr₃/rGO/α-Fe₂O₃ (mediated Z-scheme),¹¹² heterojunctions studied in the



literature, as shown in Figure 4 b. The enhanced charge separation correlates directly with the improvement in the respective photocatalytic activities. The trend holds across a wide range of heterojunction combinations – CsPbBr₃ QDs/GO,¹³ CsPbBr₃/g-C₃N₄,¹¹³ CsPbBr₃/TiO-g-C₃N₄,¹¹⁴ CsPbBr₃/MXene nanosheets (Ti₃C₂T_x),¹¹⁵ CsPbBr₃/N-doped carbon dots,¹¹⁶ CsPbBr₃ QDs/Bi₂WO₆ nanosheet,¹¹⁷ FAPbBr₃/Bi₂WO₆,¹¹⁸ CsPbBr₃/CdS,¹¹⁹ ZnSe nanorods/CsSnCl₃,¹²⁰ and Cs₃Bi₂Br₉/g-C₃N₄.¹²¹ Some of these benefit from interfacial electric field that further assist in charge separation. High surface area and porous metal organic frameworks (MOFs) have also been explicitly used as charge extracting layers which are advantageous against insulating SiO₂,¹²² or inorganic/polymer matrix.¹²³ CsPbBr₃-Zeolite imidazolate (ZIF) core-shell composite,¹²⁴ MAPbI₃ QDs/PCN-221 (Fe-based porphyrin) encapsulated structure,¹²⁵ and Cs₃Bi₂Br₉ and Cs₂AgBiBr₆ nanodots/mesoporous titania facilitated enhanced electron transfer to promote photocatalytic CO₂ reduction to CO and CH₄ respectively.¹²⁶ While lifetime changes help, the unambiguous determination of charge transfer from PL kinetics requires the knowledge of carrier injection levels. This is frequently overlooked in the measurements. Thus, fluence conditions are extremely critical to unambiguously discern decay components related to charge transfer and not due to recombination activity. Moreover, subjecting to similar light illumination conditions used during the device testing would be beneficial to gain mechanistic understanding.

Another concern is regarding the steady-state PL quenching, which is also described as a marker of charge transfer process. However, PL quenching may also occur due to enhanced recombination at the interface and/or reabsorption effects from the heterojunction layer rather than charge transfer. Ideally, the heterojunction should maintain a high PL under open-circuit conditions (which is mostly the case) due to the passivating nature of the interface. This way steady-state PL is quite useful to screen the passivating interfaces. On the other hand, a rapid PL quenching should occur when deviating from open circuit conditions *i.e.*, when the charge



carriers are efficiently extracted. Considerations on energy band alignments are necessary to ensure efficient transfer of charges.

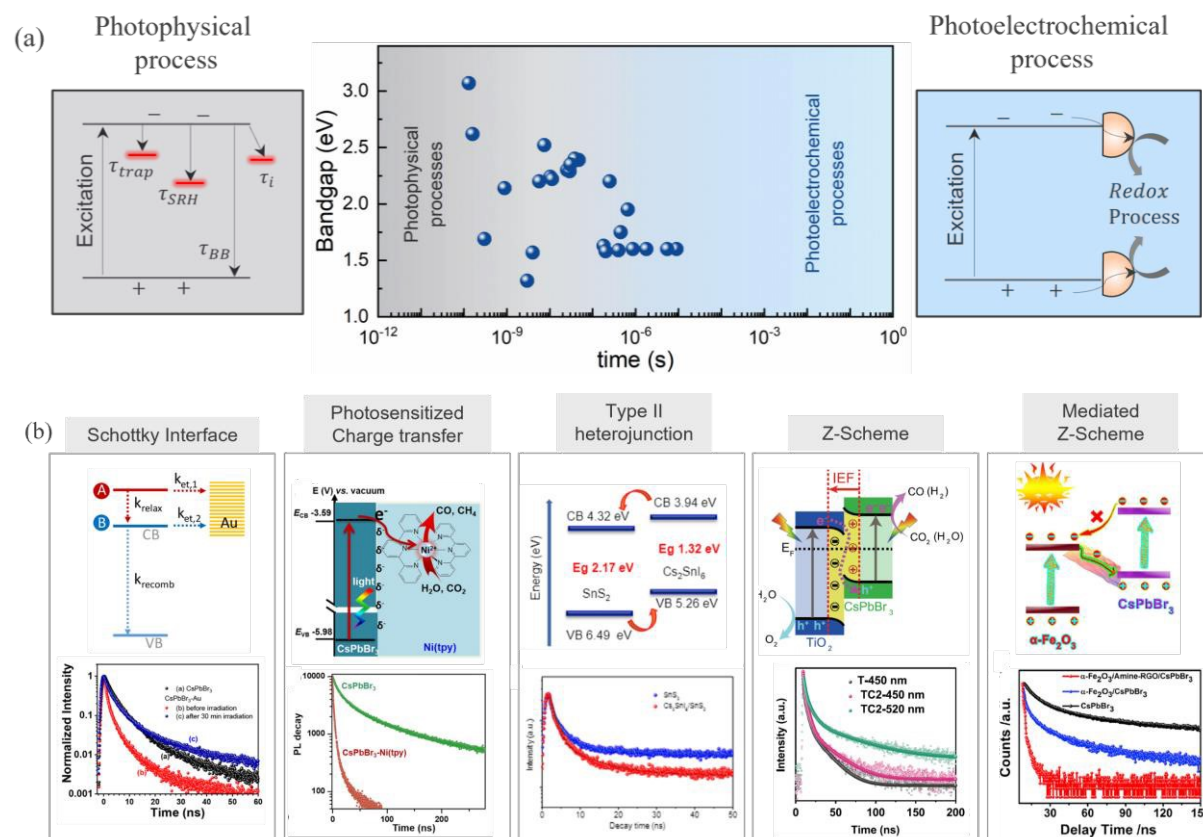


Figure 4. (a) Charge carrier lifetimes for various HaPs derived from transient photoluminescence spectroscopy. Photophysical and photoelectrochemical regimes are differentiated based on the different timescales. The data points are taken from the literature.^{95, 108-110, 112, 124-141} (b) Heterojunction schemes utilized to separate the photogenerated charge carriers and drive photoelectrochemical CO₂ reduction from HaPs. Schottky interface, Reprinted with permission from ref¹⁰⁷. Copyright 2021 American Chemical Society. Photosensitized charge transfer, Reprinted with permission from ref¹⁰⁸, Copyright 2021 American Chemical Society. Type II heterojunction, Reprinted with permission from ref,¹⁰⁹ Copyright 2019 American Chemical Society. Z-Scheme, Reproduced from ref¹¹⁰, Copyright



2020 Nature Publishing Group. Mediated Z-Scheme, Reproduced from ref^{11,12}, Copyright 2020 Cell Press. Open Access Article Online
DOI: 10.1039/D4CY00091A

2.2 Charge separation and its utilization for catalysis

Despite plethora of experimental demonstrations, the fundamental understanding remains unclear regarding how separated charge carriers participate in the catalytic reaction. How many separated charge carriers indeed participate in the photocatalytic reaction and determine the Faradaic efficiency? How do surface traps/defects influence the surface charge and photocatalytic activity? What is the effect of charge separation on stability? These questions can be partially addressed by in-situ and operando spectroscopic techniques such as photoluminescence, transient absorption, and impedance spectroscopy, which can provide valuable mechanistic insights with high spatial resolution.

The success of defect passivation and charge transport layers in HaPs based solar cells has not been translated to photoelectrochemical devices. In-situ studies can provide mechanistic insights on charge transfer at the complex HaPs/electrolyte interface and determining the rate limiting step. Multilayered tandem architectures and selective co-catalyst integration should be explored to maximum charge transfer efficiency. Thus, minimization of energy loss should be considered at every interface. Recent demonstrations on the possibility of hot carrier extraction in particulate HaPs photocatalysts expand the capabilities of these materials.

3. Photocatalytic Reactions on Halide Perovskites

3.1 Engineering morphology and dimensionality for enhanced photocatalytic performance

HaPs morphology and dimensional engineering have shown to influence the photocatalytic activity through change in the local electronic structure induced by surface coordination environment, catalytic reaction sites, surface charge density, binding energy of CO₂ and



intermediates, and surface area. In terms of morphology, quantum confined HaP structures have been explored in photocatalysis, such as QDs (0D), nanorods/nanowires (1D), nanosheets/nanoplatelets (2D), and nano/microcrystals crystals (> 100 nm, 3D).¹⁴² Nanocrystalline HaPs show enhanced photocatalytic activity owing to their high surface-to-volume ratio and demonstrate more resilience to phase transformations. However, they tend to be less

stable compared to their bulk counterparts. Specific advantages and opportunities for nanocrystalline HaPs include suppressed phase segregation, exploitation of hot carriers, high surface area. On the other hand, charge carrier extraction is challenging in such nano dimensional systems due to the excitonic nature of the optical excitations as evidenced from high PL quantum yields (PLQY) and lower lifetimes. An additional challenge comes from charge transport limitations as many of the QDs are coated with insulating ligands. Hence, the efficiency of perovskite QD solar cells are far lesser than perovskite thin film solar cells. A comparative view based on important metrics for photocatalysis for single crystals, thin films and nanoparticles are shown in Figure 5.

Lowering the dimensionality leads to a higher surface area which is beneficial for catalytic charge transfer. Study on nanocrystal size dependence showed higher photocatalytic activity and stability for 8.5 nm quantum confined nanocrystal, leading to longer PL lifetime of 9.7 ns.¹⁴³ Two dimensional (2D) layered structures provide better conducting pathways for charge transfer due to the large interfacial area. For instance, Jiang *et al.* fabricated heterojunction from CsPbBr₃/Bi₂WO₆ 2D sheets for CO₂ reduction,¹⁴⁴ where higher interface area of 2D sheet

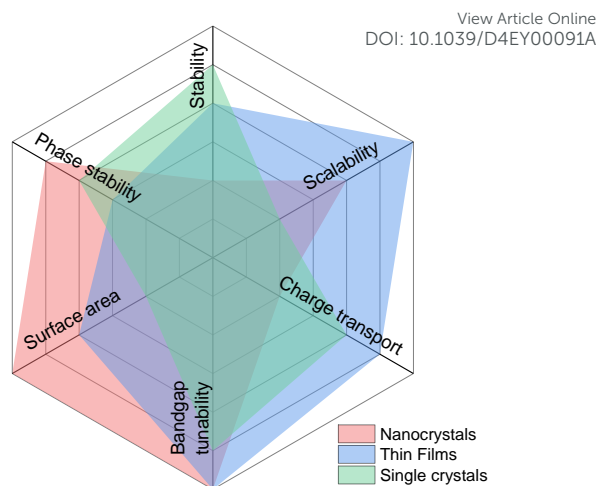


Figure 5. (a) Radar chart depicting the comparison of different metrics for nanocrystals, thin films, and single crystals HaP-based photocatalytic systems.



led to 5-fold increase in CO₂ conversion yield compared bare CsPbBr₃ nanosheets (Figure 6 a).

c). Functionalization of a co-catalyst can further help in boosting the photocatalytic activity.

However, maintaining structural integrity of co-catalyst on the support and avoiding

precipitation during the photocatalytic reaction is extremely daunting.¹⁴⁵ The improvements

from nano sizing, although seemingly obvious, need to be rationalized for long term

performance. Research work from Zhu *et al.* critically assessed the viability of CsPbBr₃

nanoparticles having different sizes (4 nm to 24 nm) for organic transformation, as shown in

Figure 6 d and e. They observed that while faster photocatalytic activity is observed initially

for smaller HaP nanocrystals, the overall yield remained less than larger nanocrystals in long

term operation.¹⁴⁶ (Figure 6 f)

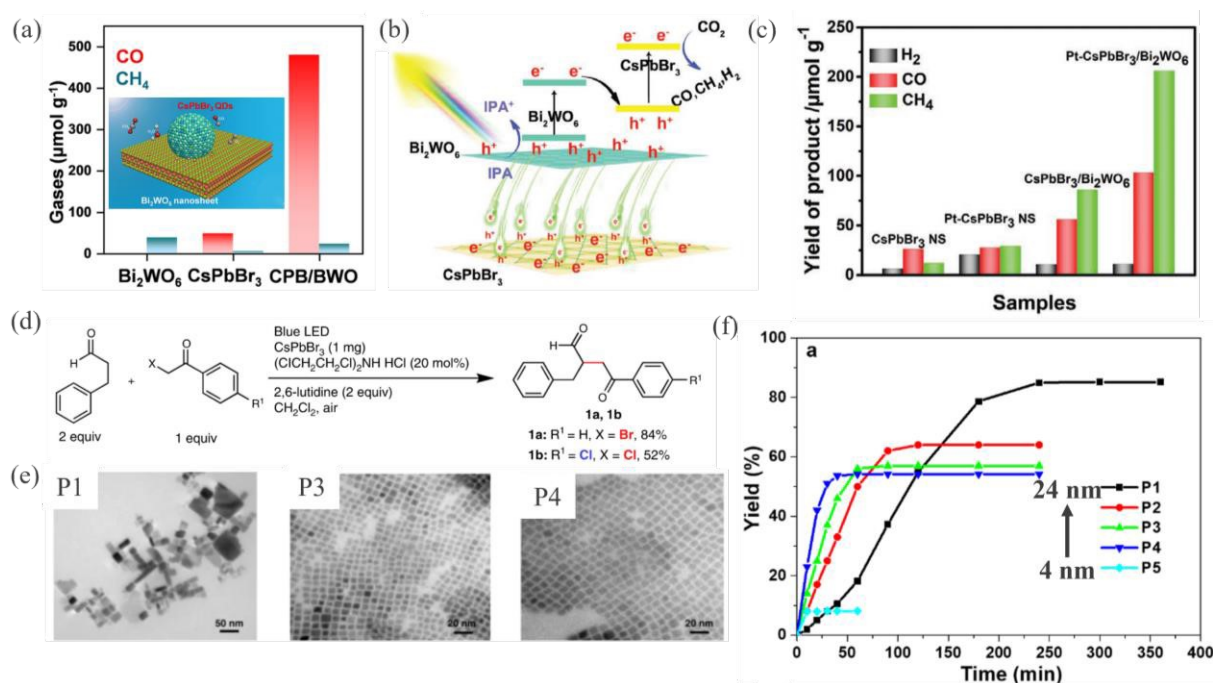


Figure 6. (a) Product yield during the CO₂ photoreduction/H₂O photooxidation over 0D/2D

CsPbBr₃/Bi₂WO₆ and its individual components. Inset shows the schematic illustration of

CsPbBr₃ zero-dimensional (0D) nanocrystals. Reprinted with permission from ref¹¹⁷.

Copyright 2020 American Chemical Society. (b) Conceptual band diagram of the 2D/2D

heterojunction depicting Z-scheme and charge carrier dynamics. (c) Product yield rates during

photocatalytic CO₂ reduction/isopropyl alcohol oxidation over the 2D/2D heterostructure



system and its individual components. Reproduced from ref¹⁴⁴. Copyright 2020 Wiley. View Article Online
DOI: 10.1039/D4CY00091A

Organic transformation reaction and the resulting product, (e) Transmission electron microscopy images of various sizes of CsPbBr₃ nanocrystals as photocatalysts. (f) Percent yield of product over time for CsPbBr₃ nanocrystals as function of nanocrystal size (P1, P2, P3, P4 and P5 refer to 24 nm, 14 nm, 9 nm, 6 nm, and 4 nm respectively). Reproduced from ref¹⁴⁶. Copyright 2019 Nature Publishing Group.

3.2 Exploitation of different crystal shapes and facets

Synthesis of different shapes of halide perovskite nanoparticles offers new opportunities in photocatalysis. Reasonable success has been achieved in synthesizing shape-controlled nanoparticles, such as facile room temperature synthesis of CsPbX₃ nanoparticles.¹⁴⁷ Since halide perovskites have long electron and hole diffusion lengths, the anisotropy in the crystal structure can lead to different electron and hole migration pathways which can help in spatial decoupling of the reduction and oxidation reactions. Li *et al.* have showed migration of holes and electrons to the edge (100) and (006) basal facets, respectively, on Cs₃Bi₂I₉ hexagonal prisms, using Co²⁺ (for oxidation) and Pt⁴⁺ (for reduction) as redox probes, as shown in Figure 7a.¹⁴⁸ Different atomic arrangements on crystal facets dictate the surface energy and the interaction with the reaction environment. Selective functionalization of co-catalysts over crystal planes that have reduced kinetic barriers for photocatalytic CO₂ reduction is highly interesting. This strategy has recently showed quantum efficiency approaching 100 % for photocatalytic water splitting reaction by selectively functionalizing Rh/Cr₂O₃ at (100) and CoOOH at (110) facet of SrTiO₃-Al nanoparticle as HER and OER co-catalyst, respectively.¹⁴⁹ Similarly, taking advantage of the crystallographic anisotropy, pseudo type-II facet selective CsPbBr₃- sulfobromide Pb₄S₃Br₂ epitaxial heterostructures have been demonstrated to improve the catalytic activity, Figure 7b.



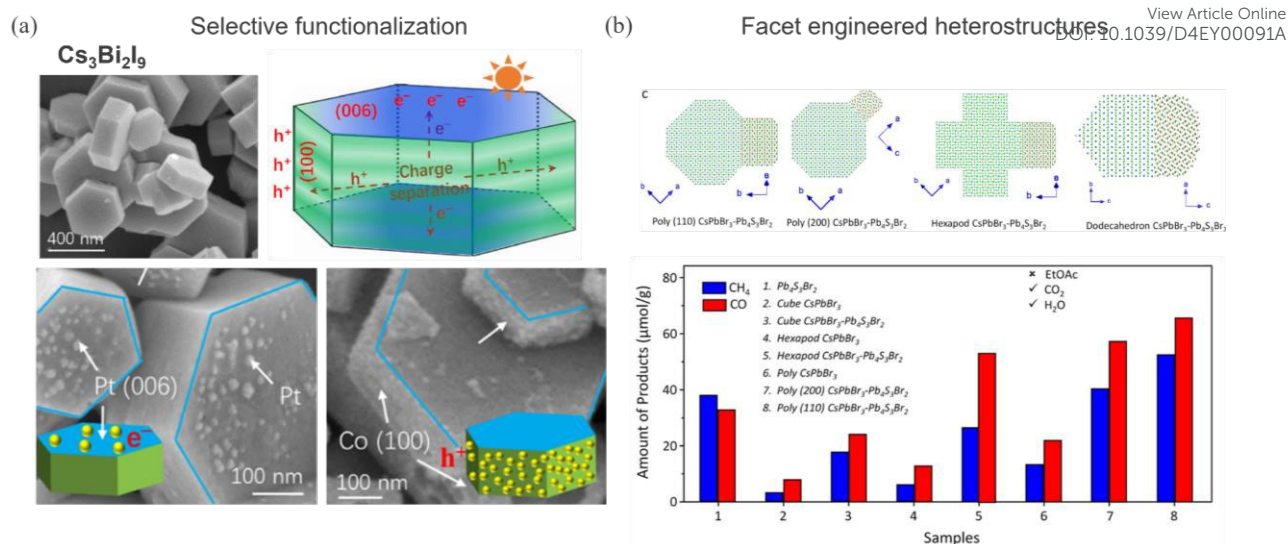


Figure 7. (a) Anisotropic charge transport pathways leading to distinct interaction at (100) and (006) facets of $\text{Cs}_3\text{Bi}_2\text{I}_9$ hexagonal prisms. Reprinted with permission from ref¹⁴⁸. Copyright 2022 American Chemical Society (b) Atomic models of CsPbBr_3 -sulfobromide $\text{Pb}_4\text{S}_3\text{Br}_2$ heterostructures of different shapes: rhombicuboctahedron, hexapods, and dodecahedron nanostructures. (Bottom) Products distribution after 2h of photocatalytic reaction for different heterostructure shapes under CO_2 -saturated H_2O vapor. Reprinted with permission from ref¹⁵⁰. Copyright 2022 American Chemical Society.

In a recent study, albeit for solar cells, it is shown that (111) facet dominated FAPbI_3 film is more stable against moisture and phase transition, which the authors attributed to the reduced chemisorption/interaction strength of water molecules on (111) facet compared to more (100) facet that is predominant in conventional thin films.¹⁵¹ These studies clearly suggest the importance of facet engineering to achieve high performing and stable photocatalytic devices.

3.3 Activation and manipulation of catalytically active sites

Catalytically active sites are essential for desired reduction and oxidation activity. The intrinsic activity of the active sites depends on inherent electronic structuring and surface atomic arrangements that affect the adsorption and desorption of reactive intermediates. Exposing



active sites over the surface and enhancing their accessibility for the reactants could modulate photocatalytic performance. Apart from poor stability in electrolytes, HaP also suffers from lack of highly active sites for desired reactions.¹⁵² Various strategies, such as morphology engineering, surface/interface structuring, heterojunction construction, encapsulation methodologies, and pairing co-catalysts, are explored to enhance the activity of HaP photocatalysts. For instance, Y.-F. Xu *et al.*, reported the development of CsPbBr₃ nanocrystal/palladium nanosheet (CsPbBr₃NC/Pd NS) composites for improved photocatalytic CO₂ reduction in water vapor.¹⁵³ This study revealed that even though the pristine CsPbBr₃ nanocrystals displayed an activity for CO₂ reduction, the performance could be significantly enhanced by integrating with Pd nanosheets (photoelectron consumption rate increased from 9.86 to 33.9 $\mu\text{molg}^{-1}\text{h}^{-1}$). Such a performance enhancement could be stemmed in fact that the creation of metal/semiconductor Schottky contact between Pd NS and CsPbBr₃ NCs should accelerate the charge separation and transfer properties along with exposure of catalytically active Pd sites.

Employing the binding sites on HaP to immobilize catalytically active species can assist in achieving high reaction activity of HaP-based hybrid photocatalysts. For example, Z. Chen and co-workers stabilized [Ni(terpy)₂]²⁺ (Ni(tpy)) metal complex on inorganic ligand-capped CsPbBr₃ NCs to form CsPbBr₃-Ni(tpy) hybrid photocatalyst.¹⁰⁸ Apart from providing active Ni(tpy) catalytic centers, the metal complexes also served as electron sinks by accepting photoexcited electrons from HaP nanocrystals and thus suppressing electron-hole recombination. Consequently, CsPbBr₃-Ni(tpy) hybrid photocatalyst yielded 1724 $\mu\text{mol/g}$ (CO/CH₄) in the reduction of CO₂, which is about 26 times higher than the yield achieved by pristine CsPbBr₃ NCs. In another work, L.-Y. Wu *et al.*, encapsulated MAPbI₃ perovskite QDs in the pores of Fe-porphyrin based metal organic framework (PCN-221(Fe_x)) through a sequential deposition procedure.¹²⁵ Utilizing steady-state and time-resolved PL measurements,



it was revealed that, due to close contact of absorber and catalysts, photogenerated electrons from MAPbI₃ QDs can easily be transferred to catalytically active sites of Fe porphyrins and thus enhance the charge separation efficiencies and activity of the resulting hybrid photocatalyst. Furthermore, metal-organic framework structures were also found to improve the stability of MAPbI₃ QDs in water-involved photocatalytic systems. Following these effects, the optimized MAPbI₃@PCN-221(Fe_x) exhibited a CO₂ reduction yield of 1559 mmol g⁻¹ (CO (34%) and CH₄ (66%)) with high stability (linear productions over 80 hours). Exploration of such strategies seems to improve the effectiveness of HaP-based photocatalysts in CO₂ reduction. However, more efforts are required to enhance the activity-stability of these newly emerged photocatalysts.

Surface active sites should be optimized in terms of their density, accessibility, and intrinsic activities. Given that the fundamental understanding of catalytic mechanisms is still limited, in-situ characterization techniques and DFT-based calculations on surface energies with considerations on intermediates should help to achieve better optimizations. For instance, the defective states in materials can be trap sites for carriers, leading to an increased rate of electron-hole pairs recombination. On the other hand, defective sites could come with increased intrinsic activity, facilitating better reaction rates. Therefore, systematic analysis and detailed investigations based on in-situ and theoretical studies help exploit the materials to off-limits. In-situ analysis also assists in revealing the dynamic surface reconstruction of catalysts during the actual testing. Further augmentation with advanced machine learning algorithms can help in rationalizing and elucidating the catalytically active sites *via* high-throughput complex calculations of site-specific reactant binding energies and reaction intermediates.

3.4 Product selectivity for CO₂R products

The product selectivity primarily depends on the surface electronic states which govern the CO₂ activation/adsorption, catalytically active sites, and intermediate adsorption/desorption



properties. Also, the availability of surface charges dictates the reaction pathways. Evidently, it is difficult to achieve reduction products that involve a higher number of electrons at the surface, such as CH₃OH and other C₂₊ products. CO and CH₄ are the major CO₂ reduction products for HaPs. The product yield for various HaPs is shown in Figure 8a and b and compared against other photocatalysts for CO₂ reduction. There is no report on methanol or higher order C₂ product yet. Success in improving CO and CH₄ production has been achieved through different heterojunction schemes, morphology, compositional and dimensional engineering, as discussed above. The relative distribution of CO and CH₄ from different heterostructures are shown in Figure 8 c. Mechanistic and theoretical insights on CO₂ activation and adsorption energy of intermediates, and proton coupled electron transfer reaction (PCET) is lacking for HaPs, contrary to oxide perovskites.

Sheng *et al.* exploited the concept of Frustrated Lewis pairs (FLP) to achieve efficient dissociation of H₂ and CO₂ reduction on Pb-free Cs₃Bi₂Br₉ and Cs₂CuBr₄ quantum dots.^{127, 129} Utilizing in situ diffuse reflectance infrared Fourier transform spectra (DRIFT) and density functional theory (DFT) calculations, the authors show that the surface catalytic sites can be regulated *via* bromine modulation and spontaneous polarization effect due to Cu-d band properties in Cs₃Bi₂Br₉ and Cs₂CuBr₄ respectively.

View Article Online
DOI: 10.1039/D4CY00091A

EES Catalysis Accepted Manuscript



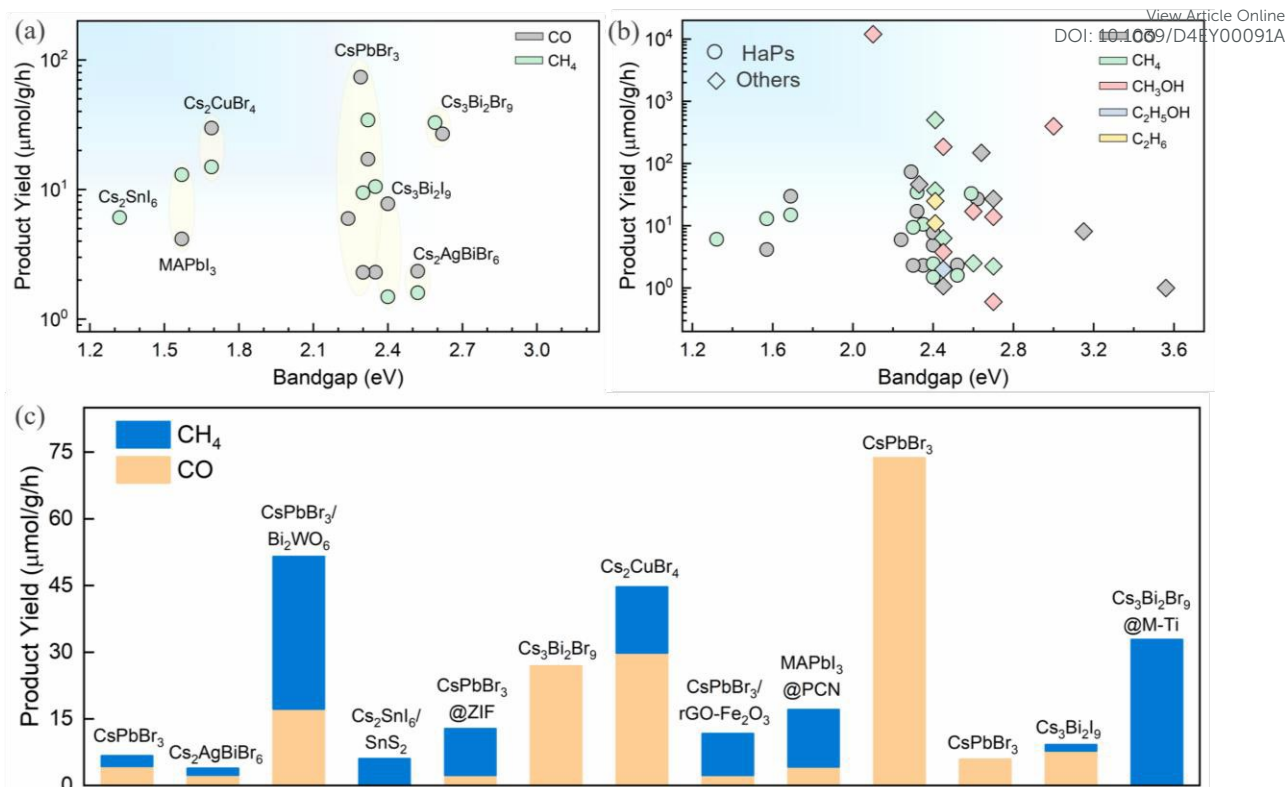


Figure 8. (a) Product yield during photocatalytic CO₂ reduction for various perovskites, (b) Comparison of products and their respective yield for HaPs and other semiconductors,^{16, 113, 154-166} (c) Product distribution from different perovskites and perovskite heterojunctions.^{13, 109, 110, 112, 124-129, 137, 139, 144}

The estimation of the energetic barrier and binding strengths of key intermediates such as CO*, COOH* and CH₄* species on perovskite surfaces are critical to alter and design surfaces that can steer the reaction kinetics in different hydrogenation pathways. Studies combining in-situ experiments and theory can be extremely valuable to achieve breakthroughs in the field.

4. Improvements in stability enabling advanced photoelectrochemical devices

Poor stability of perovskite based photoelectrodes in PEC type devices limits its potential due to the reduction in the photovoltage output over time. The photovoltage loss incurred due the degradation reduces the solar-to-fuel conversion efficiency. Both intrinsic (ion migration, defects and traps, phase instability) as well extrinsic environmental stresses act to as trigger or accelerate degradation. Adequate bulk and surface passivation schemes through additive



engineering, molecular passivation, and barrier layers have drastically improved the stability of perovskite devices with minimal photovoltage loss.¹⁶⁷⁻¹⁶⁹ Additionally, applying an external encapsulation layer and/or changing the chemical environment improves the operational stability of perovskite photoelectrodes in aqueous media, providing an extended window to drive various reduction and oxidation reactions.

4.1 Perovskite based photocathodes for reduction reactions

The most widely explored CsPbBr₃ had an average carrier lifetime in the range of 1 – 50 ns, which is significantly lower than the HaPs used in best performing solar cells. This is owing to the aqueous instability issues associated with HaP compositions used in solar cells. The chemical bonding in HaPs is highly ionic in nature, which causes instability in polar solvents and liquid electrolytes. This is usually mitigated by exploiting dynamic precipitation-solubility equilibrium in HX acid solution,¹⁷⁰ or using purely organic or mixed aqueous-organic solvents.^{117, 144} Therefore, alternative oxidation of organic compounds is advantageous both with regards to stability and energetics. Ethyl acetate, isopropyl alcohol and benzyl alcohol have been used for oxidative half reaction. This provides an opportunity for synthesizing a wide range of value-added chemicals. However, the practical and economic benefit of utilizing these chemicals must be assessed in advance.

Additive engineering and site-specific molecular passivation routes have also been quite successful in achieving long term stability of perovskites in PV devices while simultaneously addressing the ion/halide migration issues. Encouraging device modifications have been proposed to make them stable in different photoelectrochemical environments. As an example of an integrated system, Liang *et al.* demonstrated carbon encapsulated MAPbI₃ perovskite solar cells sealed by an electrode integrated with catalyst layer for photoelectrochemical water splitting.¹⁷¹ Recently, direct integration of catalyst on photocathode/photoanodes have been possible, thanks to passivating and conductive carbon layer.



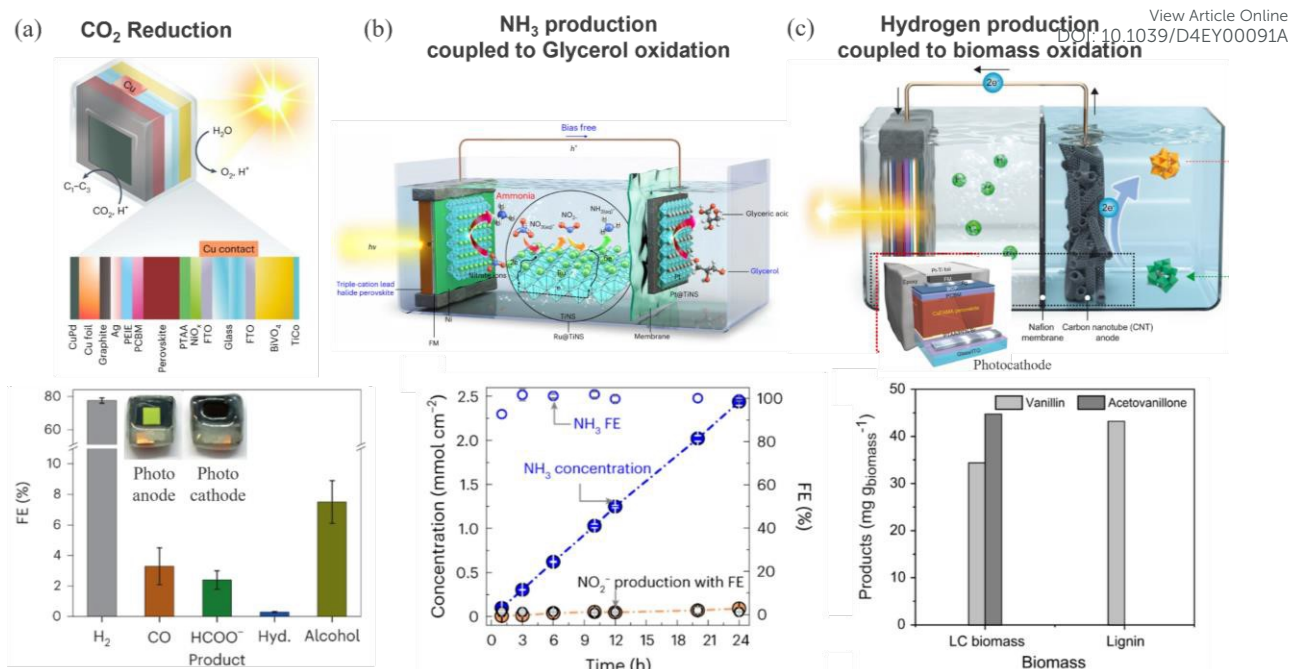


Figure 9. (a) Schematic representation of a wireless standalone BiVO₄-perovskite artificial leaf like device and corresponding Faradaic efficiency of various products after photocatalytic CO₂ reduction. Reproduced from ref¹⁷². Copyright 2023 Springer Nature Limited. (b) Schematic of the perovskite photocathode-based PEC cell used for NH₃ production. Bottom graph shows the amount of NH₃ generated for Ru@TiNS/Ni/perovskite photocathode - Pt@TiNS anode device for simultaneous nitrate reduction and Glycerol oxidation. Reproduced from ref¹⁷³. Copyright 2024 Springer Nature Limited. (c) Schematic of the perovskite PEC device for hydrogen generation at photocathode and biomass oxidation at anode. Bottom figure shows the production of vanillin and acetovanillone from lignocellulosic biomass, lignin, hemicellulose, and cellulose oxidation. Reproduced from ref¹⁷⁴. Copyright 2022 Springer Nature Limited.

Fehr *et al.* showed solar driven water splitting from a mixed cation Cs_{0.05}FA_{0.85}MA_{0.1}Pb(I_{0.95}Br_{0.05})₃ (photocathode) and FA_{0.97}MA_{0.03}PbI₃ (photoanode) perovskite solar cell directly integrated with carbon electrode having overall STH efficiency of 20.8%.¹⁷⁵



For CO₂ photoelectrochemical reduction, Andrei *et al.* demonstrated the success of carbon encapsulation approach to fabricate a monolithic triple cation (CsFAMA)PbI_{3.2}Br_{0.66} based perovskite-BiVO₄ tandem PEC as standalone system for CO₂ reduction (see Figure 9a).^{30, 172, 176} Carbon encapsulation provides a distinct avenue to extend the applicability of wider perovskite compositions in photocatalysis. In addition to carbon, Field's metal (FM) and metallic foils are also used to enhance electrical conduction and stability. For example, Tayyebi *et al.*¹⁷³ and Choi *et al.*¹⁷⁴ have demonstrated ammonia and hydrogen production respectively, from FM and metallic layer protected perovskite photocathodes, as shown in Figure 9 b and c. This way multi-layer protective layers, also serve as charge transport layers, have been successfully applied to drive different redox reactions (CO₂, nitrate, and water reduction) at high photocurrent density (~ 20 mA/cm²). The coupling of alternative oxidation reactions such as Glycerol and lignocellulosic biomass has opened a new paradigm in this direction.

4.2 Perovskite based photoanodes for oxidation reactions

Carbon encapsulation is not merely limited to reduction reactions but extended to perovskite photoanodes to drive oxidation chemistry. Excellent progress has been made in driving oxidation reactions from carbon encapsulated perovskite photoanodes. Mesoporous carbon protected FAPbBr₃ based photoanode demonstrated 8.5 % STH efficiency, surpassing the performance achieved from analogous photoanodes such as BiVO₄, Fe₂O₃, TiO₂, WO₃, Ta₃N₅.¹⁷⁷ Poli *et al.* utilized an Ir-catalyst embedded bilayer of graphite sheet and mesoporous carbon electrode protected inorganic CsPbBr₃ photoanode for water oxidation.¹⁷⁸ Stability and activity can be further improved modulating surface chemistry and catalyst engineering. Depending on the electrochemical response of organic ligands and metallic catalysts, the redox ability of HaP-based materials can be tuned to yield value-added compounds with reduced energy input.



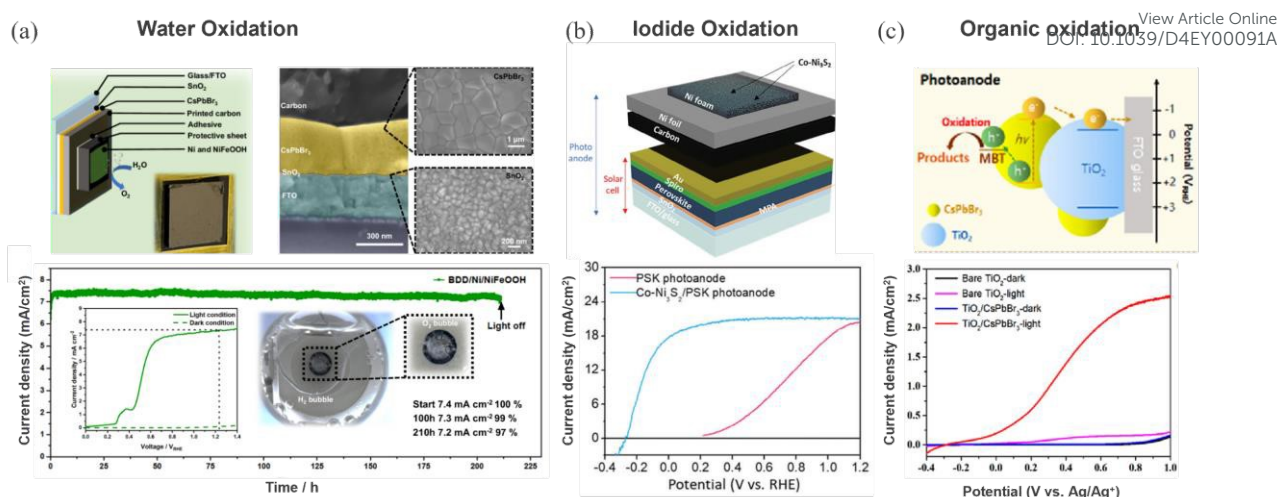


Figure 10. (a) Water oxidation: CsPbBr₃ photoanode protected with GC/Ni/NiFeOOH and corresponding cross-sectional and top-view SEM micrographs of the device stack. Bottom shows the device stability testing at +1.23 V_{RHE} under 1 sun illumination. Inset shows the voltammogram under 1 sun (solid line) and in dark (green dashed line) and photograph of the photoanode under operation showing the evolved O₂ bubbles. Reproduced from ref.¹⁷⁹ Copyright 2024 Springer Nature Limited. (b) Iodide oxidation: Device structure of the perovskite photoanode showing Co-Ni₃S₂/Ni foam/Ni foil/carbon powder stacked on solar cell structure and corresponding voltammogram under 1-sun illumination ins in 0.5 M KPi electrolyte containing 0.5 M KI. Reproduced from ref.²⁴ Copyright 2024 Wiley. (c) Organic oxidation: Perovskite photoanode based PEC cell for MBE oxidation and below shows the LSV scans of the photoanodes in 0.1 M tetrabutylammonium hexafluorophosphate (Bu₄NPF₆) in dichloromethane (DCM) with 0.05 M MBT. Reprinted with permission from ref.¹⁸⁰ Copyright 2023 American Chemical Society.

Recently, Zhu *et al.* have achieved remarkable stability of 210 h for water oxidation in aqueous electrolyte through encapsulating with electrocatalytically active glassy carbon and boron doped diamond sheets containing earth abundant NiFeOOH catalyst.¹⁷⁹ Similar catalyst has been integrated to a high performing FAPbI₃ based photoanode to realize an impressive 8.5 % solar-to-hydrogen (STH) on a scaled-up 123 cm² mini modules.¹⁸¹ Recent demonstrations on



heterojunctions based on conjugated polymers with metal sulfide (Sb_2S_3),¹⁸² metal oxide (Mo:BiVO_4),¹⁰³ and metal nitride (Ta_3N_5)¹⁰⁴ can serve as a basis to develop perovskite photoanode with carrier extraction efficiency. Beyond water oxidation, few studies explore perovskite photoanodes for alternative oxidation reactions such as iodide oxidation and organic transformations for environmental remediation. Iodide oxidation reaction (IOR) has thermodynamically lower energetic requirement and is kinetically more favorable and OER. Yun *et al.* have developed Co- Ni_2S_3 catalyst embedded in carbon matrix and integrated to standard n-i-p perovskite solar cell stack to realize photoanodes for IOR. Figure 10 b shows the photoanode device configuration and corresponding voltammogram with and without catalyst. The protected photoanode stack yielded a STH efficiency of 11.45 % along with a stable 25 h of continuous operation.²⁴ Climent *et al.* demonstrated reversible photoelectrochemical transformation of Benzyl alcohol (BzOH) to benzyl aldehyde (BzCHO) and vice versa using selective charge transfer scheme, i.e. $\text{TiO}_2/\text{CsPbBr}_3$ for oxidation and $\text{NiO}/\text{CsPbBr}_3$ for reduction.¹⁸³ The same group later extended the approach to drive oxidation of organic pollutant such as 2-mercaptobenzothiazol (MBA) using Al_2O_3 protected CsPbBr_3 photoanode, as shown in Figure 10 c.¹⁸⁰ The efficiency of the process was further enhanced by externally powering the PEC device with perovskite PV module.

5. Emerging concepts

While vast majority of perovskites remain unexplored for photocatalytic application, high-throughput combinatorial screening and DFT augmented machine learning provide immense opportunities to discover stable and catalytically active perovskite compositions. Notable efforts are already being made in this direction to discover unique perovskite compounds for specific optoelectronic devices.¹⁸⁴⁻¹⁸⁷ The optoelectronic and photocatalytic performance descriptors discussed above can guide in refining the compositional library. Advance computational methods can also help in understanding the complex and multistep



photoelectrocatalysis process involving various interdependent parameters such as charge transfer, CO₂ activation, catalytic sites, reaction intermediates and competing reactions. In a recent attempt, Caruso *et al.* demonstrated the importance of choosing the correct descriptor for optimizing photocatalytic property. They combined machine learning models with the DFT and found that Zn²⁺ metal substitution at B-site in Cs₂AgBiBr₆ perovskite enhances the photoactivity due to optimum electronic structure, especially d-orbital configuration (d¹⁰).¹⁸⁸ The vast library of compositionally feasible perovskite compounds remained explored. The rapid rise in the computation capabilities to screen, predict and rationalize materials properties has opened new avenues to discover stable and non-toxic perovskite or perovskite inspired compounds targeted for specific photoelectrochemical processes. Moreover, the accelerated testing platforms, also known as the *laboratory of the future*, can be a powerful tool for rapid screening of compositionally and operationally stable compounds. Expanding the scope of reactions from reduction to alternative oxidation reaction is gaining interest to cover wider aspects of photoelectrochemical transformations. It is important to recognize that specific HaPs might be more suitable for certain reactions and testing conditions (pH, temperature, and irradiation etc.).

6. Outlook and Future Directions

Despite significant milestones achieved for optoelectronic devices (photovoltaics, photodetectors, lasers, LEDs etc.), the full potential of halide perovskites remains untapped for photocatalysis application. The photochemical performance and stability are far from its practical usage. In this perspective, we have emphasized fundamental concepts and examined key advancements propelling halide perovskites for photocatalysis. Promising paths are identified for future advancements and valorization of perovskite based photocatalytic systems.

(i) Targeting stable compositions and measurement conditions. Stability of the photoelectrodes is one of the biggest challenges faced in a photoelectrochemical process. To



date, archetypical MAPbI₃ and wide bandgap CsPbX₃ perovskite compositions are the most widely explored photocatalytic processes. Screening of large number of compositions with suitable bandgaps for both reduction and oxidation reaction can accelerate the development of interesting candidates and help in identifying which composition modifications lead to higher stability. With rapidly advancing materials development initiatives, there is an urgent need for a perovskite materials database, combining theory and experiments, specific for photoelectrochemical processes. This will also lead to the discovery of more robust, stable, and Pb-free compositions suitable for photocatalysis. There is a need to critically define the optimum reaction conditions such as – pH, temperature, and consider the viability of driving complete reaction at lower overpotentials with high production rate. External strategies such as Facet engineering, novel protective coatings (oxide/metal/organic) and structural engineering approaches (like core-shell structures, MOF-based encapsulation, etc.) must be developed and explored to stabilize perovskites in electrolytes. Apart from developing protective materials, their deposition/coating strategies, growth mechanisms, effects on perovskites, and photoelectrochemical activity should be investigated and understood in-depth.

(ii) Better charge transfer schemes for enhanced photocurrent. Leveraging upon the successful passivation schemes used for aqueous water splitting and CO₂ reduction, further improvement in performance can be achieved through better charge collection. In this regard, alternative heterojunctions beyond conventional electron and hole transport layers need to be developed, particularly Z-scheme configurations. Z-scheme with an optimum combination of bandgap (1.6 eV, top cell and 1.1 eV bottom cell) not only enhances the light absorption but also enhances the photo reduction/oxidation ability. Developing high surface area textured surfaces can further enhance the charge collection with better light management.

(iii) Driving alternative reactions for value added chemicals. Owing to the instability in water based aqueous media, perovskites are stabilized in alternative media, mainly, saturated



hydrohalic acids (HX; HI, HBr) solutions. The resulting product from HX splitting, H_2 and Br_2 are useful products for hygiene and energy industries. Moreover, exploring alternative anodic oxidations to OER is desirable to lower the PEC energy requirements. Halide oxidation is thermodynamically more favorable over OER and requires less kinetic overpotential due to 2-electrons involved in the reactions compared to four electrons for water oxidation. Coupling alternative reactions such as oxidation of biomass derived organic compounds (lignin, glucose, furfural, 5-hydroxymethyl furfural; HMF, glycerol, etc.) and chemical wastes (polyethylene terephthalate; PET, glyceric acid, wastewater remediation). The oxidation byproducts of these reactions include several high value chemicals such as – FDCA, dimethoxydihydrofuran, Vanillin, Glycolic acid, etc. This approach holds significant potential in reducing energy input of the paired electrochemical process, enhancing the overall techno-economic viability, and maximizing the return of energy investments. Integration of high selectivity metal complex (Ni, Fe, Ru, Ir) based molecular catalysts and (bi-) metallic (Au, Pt, Pd) co-catalysts is a promising direction to enhance the functionality of the perovskite photocatalysts. The future endeavors must eventually go beyond the above and cover additional important reactions like seawater splitting and wastewater treatment.

(iv) Towards higher order carbon compounds. A higher photovoltage is desirable to overcome overpotential losses associated with photoelectrochemical CO_2 reduction. Inspiration from photovoltaic architectures might be useful to engineer novel integration methods enhancing charge extraction and stability. High photovoltage from encapsulated and integrated perovskite PEC devices have shown promising results for unbiased standalone operation. Semitransparent perovskite PV devices can provide extra photovoltage without compromising the total photon flux. Next, overcoming mass transport limitations associated with CO_2 electrolysis, an integrated perovskite device with flow reactor and catalyst loaded gas diffusion electrode (GDE) flow reactors will pave the way for standalone PEC device at high



current densities. Surface reaction kinetics can be tuned by changing adsorption strengths of the intermediates. Advanced *in-situ* characterization tools such as – synchrotron-based techniques X-ray scattering and photoelectron spectroscopy and are helpful in identifying surface adsorbates and catalytic sites. Moreover, observation of catalytic transient states and charge transfer processes using ultrafast infrared and pump-probe spectroscopy bring exciting opportunities to understand the physical origin of the electrochemical processes at perovskite surface.

(v) Scalability challenges. From a practical perspective, the scalability aspects should be considered in the beginning itself. The facile low temperature synthesis position perovskites in a favorable scenario to develop large scale processes compared to other photocatalysts, especially oxides. While nanoparticle photocatalysts show great promise, they are confronted with scaling issues. The development of thin films artificial leaf like devices are excellent in this regard while keeping the fundamental tenets of nanoparticles and even single crystals intact. Device scalability depends also on optimizing other important components such as reactant solubility limits, mass transport limitations and the design of the reactor.

Further development lies in understanding the charge transfer processes in widely utilized heterojunction schemes, specifically perovskite-electrolyte interface. To further expand the scope of halide perovskite based photocatalytic systems, utilization of other forms of CO₂ and targeting alternative oxidation reactions is indispensable.

View Article Online
DOI: 10.1039/D4EY00091A



Author Contributions

View Article Online
DOI: 10.1039/D4EY00091A

S. Shukla: conceptualization, writing – original draft.

V. Jose, S. Shukla: reviewing and editing.

N. Mathews: conceptualization, supervision, reviewing and editing.

Conflicts of interest

There are no conflicts to declare.

Acknowledgements: SS acknowledges funding from the European Union's Horizon Europe program under the Marie Skłodowska-Curie Grant Agreement No. 101067667. SS and VJ acknowledge Catalisti VLAIO (Vlaanderen Agentschap Innoveren & Ondernemen) for their funding through the Moonshot SYN-CAT project (HBC.2020.2614), and the Belgian federal government through the Energy Transition Fund for T-REX project. N.M. would like to acknowledge the funding from National Research Foundation (NRF), Singapore, under its Competitive Research Program (CRP) (NRF-CRP25-2020-0002). The authors would like to thank Dr. Tom Aernouts and Prof. Bart Vermang for fruitful discussions.

References

1. S. Chu and A. Majumdar, *Nature*, 2012, **488**, 294-303.
2. B. Obama, *Science*, 2017, **355**, 126-129.
3. M. Victoria, N. Haegel, I. M. Peters, R. Sinton, A. Jäger-Waldau, C. del Cañizo, C. Breyer, M. Stocks, A. Blakers, I. Kaizuka, K. Komoto and A. Smets, *Joule*, 2021, **5**, 1041-1056.
4. P. De Luna, C. Hahn, D. Higgins, S. A. Jaffer, T. F. Jaramillo and E. H. Sargent, *Science*, 2019, **364**, eaav3506.
5. E. Papadis and G. Tsatsaronis, *Energy*, 2020, **205**, 118025.
6. N. S. Lewis and D. G. Nocera, *Proc. Natl. Acad. Sci.*, 2006, **103**, 15729-15735.
7. J. M. Tarascon and M. Armand, *Nature*, 2001, **414**, 359-367.
8. A. Fujishima and K. Honda, *Nature*, 1972, **238**, 37-38.
9. M. Halmann, *Nature*, 1978, **275**, 115-116.



10. H. Nishiyama, T. Yamada, M. Nakabayashi, Y. Maehara, M. Yamaguchi, Y. Kuromiya, Y. Nagatsuma, H. Tokudome, S. Akiyama, T. Watanabe, R. Narushima, S. Okunaka, N. Shibata, T. Takata, T. Hisatomi and K. Domen, *Nature*, 2021, **598**, 304-307. View Article Online
DOI: 10.1039/D1EY00091A
11. C.-C. Yang, Y.-H. Yu, B. van der Linden, J. C. S. Wu and G. Mul, *J. Am. Chem. Soc.*, 2010, **132**, 8398-8406.
12. S. Liu, J. Li, W. Xiao, R. Chen, Z. Sun, Y. Zhang, X. Lei, S. Hu, M. Kober-Czerny, J. Wang, F. Ren, Q. Zhou, H. Raza, Y. Gao, Y. Ji, S. Li, H. Li, L. Qiu, W. Huang, Y. Zhao, B. Xu, Z. Liu, H. J. Snaith, N.-G. Park and W. Chen, *Nature*, 2024.
13. Y.-F. Xu, M.-Z. Yang, B.-X. Chen, X.-D. Wang, H.-Y. Chen, D.-B. Kuang and C.-Y. Su, *J. Am. Chem. Soc.*, 2017, **139**, 5660-5663.
14. L. Ding, F. Bai, B. Borjigin, Y. Li, H. Li and X. Wang, *Chem. Eng. J.*, 2022, **446**, 137102.
15. G. Wang, Z. Chen, T. Wang, D. Wang and J. Mao, *Angew. Chem., Int. Ed.*, 2022, **61**, e202210789.
16. Y. Wang, X. Liu, X. Han, R. Godin, J. Chen, W. Zhou, C. Jiang, J. F. Thompson, K. B. Mustafa, S. A. Shevlin, J. R. Durrant, Z. Guo and J. Tang, *Nat. Commun.*, 2020, **11**, 2531.
17. T. Kunene, L. Xiong and J. Rosenthal, *Proc. Natl. Acad. Sci.*, 2019, **116**, 9693-9695.
18. M. B. Ross, P. De Luna, Y. Li, C.-T. Dinh, D. Kim, P. Yang and E. H. Sargent, *Nat. Catal.*, 2019, **2**, 648-658.
19. D. Li, K. Yang, J. Lian, J. Yan and S. Liu, *Adv. Energy Mater.*, 2022, **12**, 2201070.
20. H. Wan, A. Bagger and J. Rossmeisl, *J. Phys. Chem. Lett.*, 2022, **13**, 8928-8934.
21. C. R. Lhermitte and K. Sivula, *ACS Catal.*, 2019, **9**, 2007-2017.
22. J. H. Montoya, L. C. Seitz, P. Chakthranont, A. Vojvodic, T. F. Jaramillo and J. K. Nørskov, *Nat. Mater.*, 2017, **16**, 70-81.
23. in *Appendix B: Tables of Physical Data. Fundamentals and Applications of Organic Electrochemistry.*, John Wiley & Sons., 2014.
24. J. Yun, Y. S. Park, H. Lee, W. Jeong, C.-S. Jeong, C. U. Lee, J. Lee, S. Moon, E. Kwon, S. Lee, S. Kim, J. Kim, S. Yu and J. Moon, *Adv. Energy Mater.*, 2024, 2401055.
25. X. Deng, R. Li, S. Wu, L. Wang, J. Hu, J. Ma, W. Jiang, N. Zhang, X. Zheng, C. Gao, L. Wang, Q. Zhang, J. Zhu and Y. Xiong, *J. Am. Chem. Soc.*, 2019, **141**, 10924-10929.
26. U. Kang, S. K. Choi, D. J. Ham, S. M. Ji, W. Choi, D. S. Han, A. Abdel-Wahab and H. Park, *Energy Environ. Sci.*, 2015, **8**, 2638-2643.
27. T. Arai, S. Sato, T. Kajino and T. Morikawa, *Energy Environ. Sci.*, 2013, **6**, 1274-1282.
28. S. Y. Lee, S. Y. Lim, D. Seo, J.-Y. Lee and T. D. Chung, *Adv. Energy Mater.*, 2016, **6**, 1502207.
29. K. Sekizawa, S. Sato, T. Arai and T. Morikawa, *ACS Catal.*, 2018, **8**, 1405-1416.
30. V. Andrei, B. Reuillard and E. Reisner, *Nat. Mater.*, 2020, **19**, 189-194.
31. C. Li, T. Wang, B. Liu, M. Chen, A. Li, G. Zhang, M. Du, H. Wang, S. F. Liu and J. Gong, *Energy Environ. Sci.*, 2019, **12**, 923-928.
32. X. Zhou, R. Liu, K. Sun, Y. Chen, E. Verlage, S. A. Francis, N. S. Lewis and C. Xiang, *ACS Energy Lett.*, 2016, **1**, 764-770.
33. T. Arai, S. Sato and T. Morikawa, *Energy Environ. Sci.*, 2015, **8**, 1998-2002.
34. Y. Sugano, A. Ono, R. Kitagawa, J. Tamura, M. Yamagiwa, Y. Kudo, E. Tsutsumi and S. Mikoshiba, *RSC Adv.*, 2015, **5**, 54246-54252.
35. T. Sekimoto, H. Hashiba, S. Shinagawa, Y. Uetake, M. Deguchi, S. Yotsuhashi and K. Ohkawa, *J. Phys. Chem. C*, 2016, **120**, 13970-13975.
36. Gurudayal, J. W. Beeman, J. Bullock, H. Wang, J. Eichhorn, C. Towle, A. Javey, F. M. Toma, N. Mathews and J. W. Ager, *Energy Environ. Sci.*, 2019, **12**, 1068-1077.



37. N. C. Deb Nath, S. Y. Choi, H. W. Jeong, J.-J. Lee and H. Park, *Nano Energy*, 2016, **25**, 51-59. View Article Online
DOI: 10.1039/C6PY00091A
38. Y. J. Jang, I. Jeong, J. Lee, J. Lee, M. J. Ko and J. S. Lee, *ACS Nano*, 2016, **10**, 6980-6987.
39. H. S. Jeon, J. H. Koh, S. J. Park, M. S. Jee, D.-H. Ko, Y. J. Hwang and B. K. Min, *J. Mater. Chem. A*, 2015, **3**, 5835-5842.
40. Q. Jia, S. Tanabe and I. Waki, *Chem. Lett.*, 2018, **47**, 436-439.
41. T. Arai, S. Sato, K. Sekizawa, T. M. Suzuki and T. Morikawa, *Chem. Commun.*, 2019, **55**, 237-240.
42. T. N. Huan, D. A. Dalla Corte, S. Lamaison, D. Karapinar, L. Lutz, N. Menguy, M. Foldyna, S.-H. Turren-Cruz, A. Hagfeldt, F. Bella, M. Fontecave and V. Mougél, *Proc. Natl. Acad. Sci.*, 2019, **116**, 9735-9740.
43. M. A. Ghausi, J. Xie, Q. Li, X. Wang, R. Yang, M. Wu, Y. Wang and L. Dai, *Angew. Chem., Int. Ed.*, 2018, **57**, 13135-13139.
44. M. Schreier, F. Héroguel, L. Steier, S. Ahmad, J. S. Luterbacher, M. T. Mayer, J. Luo and M. Grätzel, *Nat. Energy*, 2017, **2**, 17087.
45. Gurudayal, J. Bullock, D. F. Srankó, C. M. Towle, Y. Lum, M. Hettick, M. C. Scott, A. Javey and J. Ager, *Energy Environ. Sci.*, 2017, **10**, 2222-2230.
46. F. Urbain, P. Tang, N. M. Carretero, T. Andreu, L. G. Gerling, C. Voz, J. Arbiol and J. R. Morante, *Energy Environ. Sci.*, 2017, **10**, 2256-2266.
47. G. M. Sriramagiri, N. Ahmed, W. Luc, K. D. Dobson, S. S. Hegedus and F. Jiao, *ACS Sustainable Chem. Eng.*, 2017, **5**, 10959-10966.
48. M. Asadi, K. Kim, C. Liu, A. V. Addepalli, P. Abbasi, P. Yasaei, P. Phillips, A. Behranginia, J. M. Cerrato, R. Haasch, P. Zapol, B. Kumar, R. F. Klie, J. Abiade, L. A. Curtiss and A. Salehi-Khojin, *Science*, 2016, **353**, 467-470.
49. M. Schreier, L. Curvat, F. Giordano, L. Steier, A. Abate, S. M. Zakeeruddin, J. Luo, M. T. Mayer and M. Grätzel, *Nat. Commun.*, 2015, **6**, 7326.
50. B. Kim, H. Seong, J. T. Song, K. Kwak, H. Song, Y. C. Tan, G. Park, D. Lee and J. Oh, *ACS Energy Lett.*, 2020, **5**, 749-757.
51. L. Q. Zhou, C. Ling, H. Zhou, X. Wang, J. Liao, G. K. Reddy, L. Deng, T. C. Peck, R. Zhang, M. S. Whittingham, C. Wang, C.-W. Chu, Y. Yao and H. Jia, *Nat. Commun.*, 2019, **10**, 4081.
52. S. Y. Chae, S. Y. Lee, S. G. Han, H. Kim, J. Ko, S. Park, O.-S. Joo, D. Kim, Y. Kang, U. Lee, Y. J. Hwang and B. K. Min, *Sustainable Energy Fuels*, 2020, **4**, 199-212.
53. W. Deng, L. Zhang, H. Dong, X. Chang, T. Wang and J. Gong, *Chem. Sci.*, 2018, **9**, 6599-6604.
54. G. Piao, S. H. Yoon, D. S. Han and H. Park, *ChemSusChem*, 2020, **13**, 698-706.
55. Z. Chen, T. Wang, B. Liu, D. Cheng, C. Hu, G. Zhang, W. Zhu, H. Wang, Z.-J. Zhao and J. Gong, *J. Am. Chem. Soc.*, 2020, **142**, 6878-6883.
56. D. Ren, N. W. X. Loo, L. Gong and B. S. Yeo, *ACS Sustainable Chem. Eng.*, 2017, **5**, 9191-9199.
57. C. Moon and B. Shin, *Discov Mater*, 2022, **2**, 5.
58. J. W. Yang, Y. J. Ahn, D. K. Cho, J. Y. Kim and H. W. Jang, *Inorg. Chem. Front.*, 2023, **10**, 3781-3807.
59. J. Hwang, R. R. Rao, L. Giordano, Y. Katayama, Y. Yu and Y. Shao-Horn, *Science*, 2017, **358**, 751-756.
60. S. Chen, T. Takata and K. Domen, *Nat. Rev. Mater.*, 2017, **2**, 17050.
61. K. Sivula and R. van de Krol, *Nat. Rev. Mater.*, 2016, **1**, 15010.
62. E. Pastor, M. Sachs, S. Selim, J. R. Durrant, A. A. Bakulin and A. Walsh, *Nat. Rev. Mater.*, 2022, **7**, 503-521.



63. H. Li, X. Jia, Q. Zhang and X. Wang, *Chem*, 2018, **4**, 1510-1537.
64. A. Iwase, S. Yoshino, T. Takayama, Y. H. Ng, R. Amal and A. Kudo, *J. Am. Chem. Soc.*, 2016, **138**, 10260-10264.
65. G. Giuffredi, T. Asset, Y. Liu, P. Atanassov and F. Di Fonzo, *ACS Mater. Au*, 2021, **1**, 6-36.
66. X. Li, Y. Sun, J. Xu, Y. Shao, J. Wu, X. Xu, Y. Pan, H. Ju, J. Zhu and Y. Xie, *Nat. Energy*, 2019, **4**, 690-699.
67. Y. Liu, M. Xia, D. Ren, S. Nussbaum, J.-H. Yum, M. Grätzel, N. Guijarro and K. Sivula, *ACS Energy Lett.*, 2023, **8**, 1645-1651.
68. J. Y. Kim, J.-W. Lee, H. S. Jung, H. Shin and N.-G. Park, *Chem. Rev.*, 2020, **120**, 7867-7918.
69. M. Ahmadi, T. Wu and B. Hu, *Adv. Mater.*, 2017, **29**, 1605242.
70. X. Y. Chin, A. Perumal, A. Bruno, N. Yantara, S. A. Veldhuis, L. Martínez-Sarti, B. Chandran, V. Chirvony, A. S.-Z. Lo, J. So, C. Soci, M. Grätzel, H. J. Bolink, N. Mathews and S. G. Mhaisalkar, *Energy Environ. Sci.*, 2018, **11**, 1770-1778.
71. Q. Zhang, Q. Shang, R. Su, T. T. H. Do and Q. Xiong, *Nano Lett.*, 2021, **21**, 1903-1914.
72. R. A. John, N. Yantara, S. E. Ng, M. I. B. Patdillah, M. R. Kulkarni, N. F. Jamaludin, J. Basu, Ankit, S. G. Mhaisalkar, A. Basu and N. Mathews, *Adv. Mater.*, 2021, **33**, 2007851.
73. F. Temerov, Y. Baghdadi, E. Rattner and S. Eslava, *ACS Appl. Energy Mater.*, 2022, **5**, 14605-14637.
74. E. Ugur, M. Ledinský, T. G. Allen, J. Holovský, A. Vlk and S. De Wolf, *J. Phys. Chem. Lett.*, 2022, **13**, 7702-7711.
75. H. Lin, C. Zhou, Y. Tian, T. Siegrist and B. Ma, *ACS Energy Lett.*, 2018, **3**, 54-62.
76. T. M. Koh, K. Thirumal, H. S. Soo and N. Mathews, *ChemSusChem*, 2016, **9**, 2541-2558.
77. Z. Li, M. Yang, J.-S. Park, S.-H. Wei, J. J. Berry and K. Zhu, *Chem. Mater.*, 2016, **28**, 284-292.
78. D. Niesner, M. Wilhelm, I. Levchuk, A. Osvet, S. Shrestha, M. Batentschuk, C. Brabec and T. Fauster, *Phys. Rev. Lett.*, 2016, **117**, 126401.
79. T. Etienne, E. Mosconi and F. De Angelis, *J. Phys. Chem. Lett.*, 2016, **7**, 1638-1645.
80. E. M. Hutter, M. C. Gélvez-Rueda, A. Osherov, V. Bulović, F. C. Grozema, S. D. Stranks and T. J. Savenije, *Nat. Mater.*, 2017, **16**, 115-120.
81. D. R. MacFarlane, P. V. Cherepanov, J. Choi, B. H. R. Suryanto, R. Y. Hodgetts, J. M. Bakker, F. M. Ferrero Vallana and A. N. Simonov, *Joule*, 2020, **4**, 1186-1205.
82. H. Huang, B. Pradhan, J. Hofkens, M. B. J. Roeffaers and J. A. Steele, *ACS Energy Lett.*, 2020, **5**, 1107-1123.
83. J. Wang, Y. Shi, Y. Wang and Z. Li, *ACS Energy Lett.*, 2022, **7**, 2043-2059.
84. P. Calado, A. M. Telford, D. Bryant, X. Li, J. Nelson, B. C. O'Regan and P. R. F. Barnes, *Nat. Commun.*, 2016, **7**, 13831.
85. K. Takanabe, *ACS Catal.*, 2017, **7**, 8006-8022.
86. H. Hempel, T. J. Savenjie, M. Stolterfoht, J. Neu, M. Failla, V. C. Paingad, P. Kužel, E. J. Heilweil, J. A. Spies, M. Schleuning, J. Zhao, D. Friedrich, K. Schwarzburg, L. D. A. Siebbeles, P. Dörflinger, V. Dyakonov, R. Katoh, M. J. Hong, J. G. Labram, M. Monti, E. Butler-Caddle, J. Lloyd-Hughes, M. M. Taheri, J. B. Baxter, T. J. Magnanelli, S. Luo, J. M. Cardon, S. Ardo and T. Unold, *Adv. Energy Mater.*, 2022, **12**, 2102776.
87. L. M. Herz, *ACS Energy Lett.*, 2017, **2**, 1539-1548.
88. L. Krückemeier, Z. Liu, T. Kirchartz and U. Rau, *Adv. Mater.*, 2023, **35**, 2300872.
89. Y. Chen, H. T. Yi, X. Wu, R. Haroldson, Y. N. Gartstein, Y. I. Rodionov, K. S. Tikhonov, A. Zakhidov, X. Y. Zhu and V. Podzorov, *Nat. Commun.*, 2016, **7**, 12253.

View Article Online
DOI: 10.1039/D4EY00091A



90. R. Brenes, D. Guo, A. Osherov, N. K. Noel, C. Eames, E. M. Hutter, S. K. Pathak, M. Niroui, R. H. Friend, M. S. Islam, H. J. Snaith, V. Bulović, T. J. Savenije and S. D. Stranks, *Joule*, 2017, **1**, 155-167.
91. T. Kirchartz, J. A. Márquez, M. Stolterfoht and T. Unold, *Adv. Energy Mater.*, 2020, **10**, 1904134.
92. O. Stroyuk, O. Raievska, J. Hauch and C. J. Brabec, *Angew. Chem., Int. Ed.*, 2023, **62**, e202212668.
93. M. Li, S. Bhaumik, T. W. Goh, M. S. Kumar, N. Yantara, M. Grätzel, S. Mhaisalkar, N. Mathews and T. C. Sum, *Nat. Commun.*, 2017, **8**, 14350.
94. J. Shamsi, A. S. Urban, M. Imran, L. De Trizio and L. Manna, *Chem. Rev.*, 2019, **119**, 3296-3348.
95. M. Abdi-Jalebi, Z. Andaji-Garmaroudi, S. Cacovich, C. Stavrakas, B. Philippe, J. M. Richter, M. Alsari, E. P. Booker, E. M. Hutter, A. J. Pearson, S. Lilliu, T. J. Savenije, H. Rensmo, G. Divitini, C. Ducati, R. H. Friend and S. D. Stranks, *Nature*, 2018, **555**, 497-501.
96. D. W. de Quilettes, S. M. Vorpahl, S. D. Stranks, H. Nagaoka, G. E. Eperon, M. E. Ziffer, H. J. Snaith and D. S. Ginger, *Science*, 2015, **348**, 683-686.
97. G. Han, T. M. Koh, J. Li, B. Febriansyah, Y. Fang, N. F. Jamaludin, Y. F. Ng, P. J. S. Rana, S. Mhaisalkar and N. Mathews, *ACS Appl. Energy Mater.*, 2021, **4**, 2716-2723.
98. G. H. Ahmed, J. K. El-Demellawi, J. Yin, J. Pan, D. B. Velusamy, M. N. Hedhili, E. Alarousu, O. M. Bakr, H. N. Alshareef and O. F. Mohammed, *ACS Energy Lett.*, 2018, **3**, 2301-2307.
99. P. J. S. Rana, B. Febriansyah, T. M. Koh, A. Kanwat, J. Xia, T. Salim, T. J. N. Hooper, M. Kovalev, D. Giovanni, Y. C. Aw, B. Chaudhary, Y. Cai, G. Xing, T. C. Sum, J. W. Ager, S. G. Mhaisalkar and N. Mathews, *Adv. Mater.*, 2023, **35**, 2210176.
100. G. Grancini and M. K. Nazeeruddin, *Nat. Rev. Mater.*, 2019, **4**, 4-22.
101. P. P. Boix, S. Agarwala, T. M. Koh, N. Mathews and S. G. Mhaisalkar, *J. Phys. Chem. Lett.*, 2015, **6**, 898-907.
102. T. M. Koh, V. Shanmugam, X. Guo, S. S. Lim, O. Filonik, E. M. Herzig, P. Müller-Buschbaum, V. Swamy, S. T. Chien, S. G. Mhaisalkar and N. Mathews, *J. Mater. Chem. A*, 2018, **6**, 2122-2128.
103. J. W. Yang, S. G. Ji, C.-S. Jeong, J. Kim, H. R. Kwon, T. H. Lee, S. A. Lee, W. S. Cheon, S. Lee, H. Lee, M. S. Kwon, J. Moon, J. Y. Kim and H. W. Jang, *Energy Environ. Sci.*, 2024, **17**, 2541-2553.
104. J. W. Yang, H. R. Kwon, S. G. Ji, J. Kim, S. A. Lee, T. H. Lee, S. Choi, W. S. Cheon, Y. Kim, J. Park, J. Y. Kim and H. W. Jang, *Adv. Funct. Mater.*, 2024, 2400806.
105. H. R. Kwon, J. W. Yang, S. Choi, W. S. Cheon, I. H. Im, Y. Kim, J. Park, G.-H. Lee and H. W. Jang, *Adv. Energy Mater.*, 2024, **14**, 2303342.
106. S. Akel, A. Kulkarni, U. Rau and T. Kirchartz, *Phys. Rev. X Energy*, 2023, **2**, 013004.
107. J. Chakkamalayath, G. V. Hartland and P. V. Kamat, *J. Phys. Chem. C*, 2021, **125**, 17881-17889.
108. Z. Chen, Y. Hu, J. Wang, Q. Shen, Y. Zhang, C. Ding, Y. Bai, G. Jiang, Z. Li and N. Gaponik, *Chem. Mater.*, 2020, **32**, 1517-1525.
109. X.-D. Wang, Y.-H. Huang, J.-F. Liao, Y. Jiang, L. Zhou, X.-Y. Zhang, H.-Y. Chen and D.-B. Kuang, *J. Am. Chem. Soc.*, 2019, **141**, 13434-13441.
110. F. Xu, K. Meng, B. Cheng, S. Wang, J. Xu and J. Yu, *Nat. Commun.*, 2020, **11**, 4613.
111. Y.-F. Mu, C. Zhang, M.-R. Zhang, W. Zhang, M. Zhang and T.-B. Lu, *ACS Appl. Mater. Interfaces*, 2021, **13**, 22314-22322.
112. Y. Jiang, J.-F. Liao, H.-Y. Chen, H.-H. Zhang, J.-Y. Li, X.-D. Wang and D.-B. Kuang, *Chem*, 2020, **6**, 766-780.



113. M. Ou, W. Tu, S. Yin, W. Xing, S. Wu, H. Wang, S. Wan, Q. Zhong and R. Xu, *Angew. Chem., Int. Ed.*, 2018, **57**, 13570-13574. View Article Online
DOI: 10.1039/C8CY00091A
114. X.-X. Guo, S.-F. Tang, Y.-F. Mu, L.-Y. Wu, G.-X. Dong and M. Zhang, *RSC Adv.*, 2019, **9**, 34342-34348.
115. A. Pan, X. Ma, S. Huang, Y. Wu, M. Jia, Y. Shi, Y. Liu, P. Wangyang, L. He and Y. Liu, *J. Phys. Chem. Lett.*, 2019, **10**, 6590-6597.
116. E. Rathore, K. Maji, D. Rao, B. Saha and K. Biswas, *J. Phys. Chem. Lett.*, 2020, **11**, 8002-8007.
117. J. Wang, J. Wang, N. Li, X. Du, J. Ma, C. He and Z. Li, *ACS Appl. Mater. Interfaces*, 2020, **12**, 31477-31485.
118. H. Huang, J. Zhao, Y. Du, C. Zhou, M. Zhang, Z. Wang, Y. Weng, J. Long, J. Hofkens, J. A. Steele and M. B. J. Roeffaers, *ACS Nano*, 2020, **14**, 16689-16697.
119. A. Kipkorir, J. DuBose, J. Cho and P. V. Kamat, *Chem. Sci.*, 2021, **12**, 14815-14825.
120. N. Li, X. Chen, J. Wang, X. Liang, L. Ma, X. Jing, D.-L. Chen and Z. Li, *ACS Nano*, 2022, **16**, 3332-3340.
121. L. Romani, A. Speltini, C. N. Dibenedetto, A. Listorti, F. Ambrosio, E. Mosconi, A. Simbula, M. Saba, A. Profumo, P. Quadrelli, F. De Angelis and L. Malavasi, *Adv. Funct. Mater.*, 2021, **31**, 2104428.
122. Q. Zhong, M. Cao, H. Hu, D. Yang, M. Chen, P. Li, L. Wu and Q. Zhang, *ACS Nano*, 2018, **12**, 8579-8587.
123. K. Ma, X.-Y. Du, Y.-W. Zhang and S. Chen, *J. Mater. Chem. C*, 2017, **5**, 9398-9404.
124. Z.-C. Kong, J.-F. Liao, Y.-J. Dong, Y.-F. Xu, H.-Y. Chen, D.-B. Kuang and C.-Y. Su, *ACS Energy Lett.*, 2018, **3**, 2656-2662.
125. L.-Y. Wu, Y.-F. Mu, X.-X. Guo, W. Zhang, Z.-M. Zhang, M. Zhang and T.-B. Lu, *Angew. Chem., Int. Ed.*, 2019, **58**, 9491-9495.
126. Q.-M. Sun, J.-J. Xu, F.-F. Tao, W. Ye, C. Zhou, J.-H. He and J.-M. Lu, *Angew. Chem., Int. Ed.*, 2022, **61**, e202200872.
127. J. Sheng, Y. He, M. Huang, C. Yuan, S. Wang and F. Dong, *ACS Catal.*, 2022, **12**, 2915-2926.
128. Y.-F. Mu, W. Zhang, G.-X. Dong, K. Su, M. Zhang and T.-B. Lu, *Small*, 2020, **16**, 2002140.
129. J. Sheng, Y. He, J. Li, C. Yuan, H. Huang, S. Wang, Y. Sun, Z. Wang and F. Dong, *ACS Nano*, 2020, **14**, 13103-13114.
130. Z. Liu, L. Krückemeier, B. Krogmeier, B. Klingebiel, J. A. Márquez, S. Levchenko, S. Öz, S. Mathur, U. Rau, T. Unold and T. Kirchartz, *ACS Energy Lett.*, 2019, **4**, 110-117.
131. M. Stolterfoht, C. M. Wolff, J. A. Márquez, S. Zhang, C. J. Hages, D. Rothhardt, S. Albrecht, P. L. Burn, P. Meredith, T. Unold and D. Neher, *Nat. Energy*, 2018, **3**, 847-854.
132. D. W. deQuilettes, S. Koch, S. Burke, R. K. Paranjy, A. J. Shropshire, M. E. Ziffer and D. S. Ginger, *ACS Energy Lett.*, 2016, **1**, 438-444.
133. I. L. Braly, D. W. deQuilettes, L. M. Pazos-Outón, S. Burke, M. E. Ziffer, D. S. Ginger and H. W. Hillhouse, *Nat. Photonics*, 2018, **12**, 355-361.
134. A. Al-Ashouri, A. Magomedov, M. Roß, M. Jošt, M. Talaikis, G. Chistiakova, T. Bertram, J. A. Márquez, E. Köhnen, E. Kasparavičius, S. Levchenko, L. Gil-Escrig, C. J. Hages, R. Schlattmann, B. Rech, T. Malinauskas, T. Unold, C. A. Kaufmann, L. Korte, G. Niaura, V. Getautis and S. Albrecht, *Energy Environ. Sci.*, 2019, **12**, 3356-3369.
135. M. Abdi-Jalebi, M. Ibrahim Dar, S. P. Senanayak, A. Sadhanala, Z. Andaji-Garmaroudi, L. M. Pazos-Outón, J. M. Richter, A. J. Pearson, H. Siringhaus, M. Grätzel and R. H. Friend, *Sci. Adv.*, **5**, eaav2012.



136. M. Abdi-Jalebi, M. Pazoki, B. Philippe, M. I. Dar, M. Alsari, A. Sadhanala, G. Diviyani, R. Imani, S. Lilliu, J. Kullgren, H. Rensmo, M. Grätzel and R. H. Friend, *ACS Nano*, 2018, **12**, 7301-7311. View Article Online
DOI: 10.1039/D4CY00091A
137. S. S. Bhosale, A. K. Kharade, E. Jokar, A. Fathi, S.-m. Chang and E. W.-G. Diau, *J. Am. Chem. Soc.*, 2019, **141**, 20434-20442.
138. A. H. Slavney, T. Hu, A. M. Lindenberg and H. I. Karunadasa, *J. Am. Chem. Soc.*, 2016, **138**, 2138-2141.
139. L. Zhou, Y.-F. Xu, B.-X. Chen, D.-B. Kuang and C.-Y. Su, *Small*, 2018, **14**, 1703762.
140. H. Huang, H. Yuan, J. Zhao, G. Solís-Fernández, C. Zhou, J. W. Seo, J. Hendrix, E. Debroye, J. A. Steele, J. Hofkens, J. Long and M. B. J. Roeffaers, *ACS Energy Lett.*, 2019, **4**, 203-208.
141. H. Wang, X. Wang, R. Chen, H. Zhang, X. Wang, J. Wang, J. Zhang, L. Mu, K. Wu, F. Fan, X. Zong and C. Li, *ACS Energy Lett.*, 2019, **4**, 40-47.
142. A. F. Gualdrón-Reyes, C. A. Mesa, S. Giménez and I. Mora-Seró, *Sol. RRL*, 2022, **6**, 2200012.
143. J. Hou, S. Cao, Y. Wu, Z. Gao, F. Liang, Y. Sun, Z. Lin and L. Sun, *Chem. - Eur. J.*, 2017, **23**, 9481-9485.
144. Y. Jiang, H.-Y. Chen, J.-Y. Li, J.-F. Liao, H.-H. Zhang, X.-D. Wang and D.-B. Kuang, *Adv. Funct. Mater.*, 2020, **30**, 2004293.
145. J. T. DuBose and P. V. Kamat, *ACS Energy Lett.*, 2022, **7**, 1994-2011.
146. X. Zhu, Y. Lin, J. San Martin, Y. Sun, D. Zhu and Y. Yan, *Nat. Commun.*, 2019, **10**, 2843.
147. S. Sun, D. Yuan, Y. Xu, A. Wang and Z. Deng, *ACS Nano*, 2016, **10**, 3648-3657.
148. M. Li, S. Xu, L. Wu, H. Tang, B. Zhou, J. Xu, Q. Yang, T. Zhou, Y. Qiu, G. Chen, G. I. N. Waterhouse and K. Yan, *ACS Energy Lett.*, 2022, **7**, 3370-3377.
149. T. Takata, J. Jiang, Y. Sakata, M. Nakabayashi, N. Shibata, V. Nandal, K. Seki, T. Hisatomi and K. Domen, *Nature*, 2020, **581**, 411-414.
150. R. Das, A. Patra, S. K. Dutta, S. Shyamal and N. Pradhan, *J. Am. Chem. Soc.*, 2022, **144**, 18629-18641.
151. C. Ma, F. T. Eickemeyer, S.-H. Lee, D.-H. Kang, S. J. Kwon, M. Grätzel and N.-G. Park, *Science*, 2023, **379**, 173-178.
152. Z.-Y. Chen, N.-Y. Huang and Q. Xu, *Coord. Chem. Rev.*, 2023, **481**, 215031.
153. Y.-F. Xu, M.-Z. Yang, H.-Y. Chen, J.-F. Liao, X.-D. Wang and D.-B. Kuang, *ACS Appl. Energy Mater.*, 2018, **1**, 5083-5089.
154. A. Li, T. Wang, C. Li, Z. Huang, Z. Luo and J. Gong, *Angew. Chem., Int. Ed.*, 2019, **58**, 3804-3808.
155. L. Wang, M. Ghossoub, H. Wang, Y. Shao, W. Sun, A. A. Tountas, T. E. Wood, H. Li, J. Y. Y. Loh, Y. Dong, M. Xia, Y. Li, S. Wang, J. Jia, C. Qiu, C. Qian, N. P. Kherani, L. He, X. Zhang and G. A. Ozin, *Joule*, 2018, **2**, 1369-1381.
156. W. Zhao, M. Ding, P. Yang, Q. Wang, K. Zhang, X. Zhan, Y. Yu, Q. Luo, S. Gao, J. Yang and Y. Xie, *EES Catal.*, 2023, **1**, 36-44.
157. S. Gao, B. Gu, X. Jiao, Y. Sun, X. Zu, F. Yang, W. Zhu, C. Wang, Z. Feng, B. Ye and Y. Xie, *J. Am. Chem. Soc.*, 2017, **139**, 3438-3445.
158. Y. A. Wu, I. McNulty, C. Liu, K. C. Lau, Q. Liu, A. P. Paulikas, C.-J. Sun, Z. Cai, J. R. Guest, Y. Ren, V. Stamenkovic, L. A. Curtiss, Y. Liu and T. Rajh, *Nat. Energy*, 2019, **4**, 957-968.
159. L. Wang, J. Wan, Y. Zhao, N. Yang and D. Wang, *J. Am. Chem. Soc.*, 2019, **141**, 2238-2241.
160. L. Hao, L. Kang, H. Huang, L. Ye, K. Han, S. Yang, H. Yu, M. Batmunkh, Y. Zhang and T. Ma, *Adv. Mater.*, 2019, **31**, 1900546.



161. P. Xia, M. Antonietti, B. Zhu, T. Heil, J. Yu and S. Cao, *Adv. Funct. Mater.*, 2019, **29**, 1900093. View Article Online
DOI: 10.1039/C9AY00091A
162. S. Sorcar, Y. Hwang, J. Lee, H. Kim, K. M. Grimes, C. A. Grimes, J.-W. Jung, C.-H. Cho, T. Majima, M. R. Hoffmann and S.-I. In, *Energy Environ. Sci.*, 2019, **12**, 2685-2696.
163. S. Sorcar, J. Thompson, Y. Hwang, Y. H. Park, T. Majima, C. A. Grimes, J. R. Durrant and S.-I. In, *Energy Environ. Sci.*, 2018, **11**, 3183-3193.
164. Z. Jiang, W. Wan, H. Li, S. Yuan, H. Zhao and P. K. Wong, *Adv. Mater.*, 2018, **30**, 1706108.
165. T. Di, B. Zhu, B. Cheng, J. Yu and J. Xu, *J. Catal.*, 2017, **352**, 532-541.
166. G. Yin, M. Nishikawa, Y. Nosaka, N. Srinivasan, D. Atarashi, E. Sakai and M. Miyauchi, *ACS Nano*, 2015, **9**, 2111-2119.
167. H. Zhu, S. Teale, M. N. Lintangpradipto, S. Mahesh, B. Chen, M. D. McGehee, E. H. Sargent and O. M. Bakr, *Nat. Rev. Mater.*, 2023, **8**, 569-586.
168. S. Shukla, T. M. Koh, R. Patidar, J. H. Lew, P. Kajal, S. G. Mhaisalkar and N. Mathews, *J. Phys. Chem. C*, 2021, **125**, 6585-6592.
169. A. Bashir, S. Shukla, J. H. Lew, S. Shukla, A. Bruno, D. Gupta, T. Baikie, R. Patidar, Z. Akhter, A. Priyadarshi, N. Mathews and S. G. Mhaisalkar, *Nanoscale*, 2018, **10**, 2341-2350.
170. S. Park, W. J. Chang, C. W. Lee, S. Park, H.-Y. Ahn and K. T. Nam, *Nat. Energy*, 2016, **2**, 16185.
171. J. Liang, X. Han, Y. Qiu, Q. Fang, B. Zhang, W. Wang, J. Zhang, P. M. Ajayan and J. Lou, *ACS Nano*, 2020, **14**, 5426-5434.
172. M. Rahaman, V. Andrei, D. Wright, E. Lam, C. Pornrungrroj, S. Bhattacharjee, C. M. Pichler, H. F. Greer, J. J. Baumberg and E. Reisner, *Nat. Energy*, 2023, **8**, 629-638.
173. A. Tayyebi, R. Mehrotra, M. A. Mubarak, J. Kim, M. Zafari, M. Tayebi, D. Oh, S.-h. Lee, J. E. Matthews, S.-W. Lee, T. J. Shin, G. Lee, T. F. Jaramillo, S.-Y. Jang and J.-W. Jang, *Nat. Catal.*, 2024, DOI: 10.1038/s41929-024-01133-4.
174. Y. Choi, R. Mehrotra, S.-H. Lee, T. V. T. Nguyen, I. Lee, J. Kim, H.-Y. Yang, H. Oh, H. Kim, J.-W. Lee, Y. H. Kim, S.-Y. Jang, J.-W. Jang and J. Ryu, *Nat. Commun.*, 2022, **13**, 5709.
175. A. M. K. Fehr, A. Agrawal, F. Mandani, C. L. Conrad, Q. Jiang, S. Y. Park, O. Alley, B. Li, S. Sidhik, I. Metcalf, C. Botello, J. L. Young, J. Even, J. C. Blancon, T. G. Deutsch, K. Zhu, S. Albrecht, F. M. Toma, M. Wong and A. D. Mohite, *Nat. Commun.*, 2023, **14**, 3797.
176. V. Andrei, G. M. Ucoski, C. Pornrungrroj, C. Uswachoke, Q. Wang, D. S. Achilleos, H. Kasap, K. P. Sokol, R. A. Jagt, H. Lu, T. Lawson, A. Wagner, S. D. Pike, D. S. Wright, R. L. Z. Hoyer, J. L. MacManus-Driscoll, H. J. Joyce, R. H. Friend and E. Reisner, *Nature*, 2022, **608**, 518-522.
177. H. Yang, Y. Liu, Y. Ding, F. Li, L. Wang, B. Cai, F. Zhang, T. Liu, G. Boschloo, E. M. J. Johansson and L. Sun, *Nat. Commun.*, 2023, **14**, 5486.
178. I. Poli, U. Hintermair, M. Regue, S. Kumar, E. V. Sackville, J. Baker, T. M. Watson, S. Eslava and P. J. Cameron, *Nat. Commun.*, 2019, **10**, 2097.
179. Z. Zhu, M. Daboczi, M. Chen, Y. Xuan, X. Liu and S. Eslava, *Nat. Commun.*, 2024, **15**, 2791.
180. S.-Y. Lee, P. Serafini, S. Masi, A. F. Gualdrón-Reyes, C. A. Mesa, J. Rodríguez-Pereira, S. Giménez, H. J. Lee and I. Mora-Seró, *ACS Energy Lett.*, 2023, **8**, 4488-4495.
181. D. Hansora, J. W. Yoo, R. Mehrotra, W. J. Byun, D. Lim, Y. K. Kim, E. Noh, H. Lim, J.-W. Jang, S. I. Seok and J. S. Lee, *Nat. Energy*, 2024, **9**, 272-284.



182. L. Wang, W. Lian, B. Liu, H. Lv, Y. Zhang, X. Wu, T. Wang, J. Gong, T. Chen and H. Xu, *Adv. Mater.*, 2022, **34**, 2200723. View Article Online
DOI: 10.1039/D4EY00091A
183. R. Fernández-Climent, A. F. Gualdrón-Reyes, M. García-Tecedor, C. A. Mesa, D. Cárdenas-Morcoso, L. Montañes, E. M. Barea, E. Mas-Marzá, B. Julián-López, I. Mora-Seró and S. Giménez, *Sol. RRL*, 2022, **6**, 2100723.
184. M. Saliba, *Adv. Energy Mater.*, 2019, **9**, 1803754.
185. Q. Sun, W.-J. Yin and S.-H. Wei, *J. Mater. Chem. C*, 2020, **8**, 12012-12035.
186. M. Ahmadi, M. Ziatdinov, Y. Zhou, E. A. Lass and S. V. Kalinin, *Joule*, 2021, **5**, 2797-2822.
187. S. Sun, A. Tiihonen, F. Oviedo, Z. Liu, J. Thapa, Y. Zhao, N. T. P. Hartono, A. Goyal, T. Heumueller, C. Batali, A. Encinas, J. J. Yoo, R. Li, Z. Ren, I. M. Peters, C. J. Brabec, M. G. Bawendi, V. Stevanovic, J. Fisher and T. Buonassisi, *Matter*, 2021, **4**, 1305-1322.
188. X. Li, H. Mai, J. Lu, X. Wen, T. C. Le, S. P. Russo, D. A. Winkler, D. Chen and R. A. Caruso, *Angew. Chem., Int. Ed.*, 2023, **62**, e202315002.



- No primary research results, software or code have been included and no new data were generated or analysed as part of this review.

[View Article Online](#)

DOI: 10.1039/D4EY00091A

